Chapter 5: RESULTS AND DISCUSSION

5.1 Introduction

This section describes the result and discussion of acquired data from five various mines as described earlier. This section contains a description of the main finding of the research and interpretation of the results for the readers and provides the significance of the findings. After recording datasets, these were processed and analyzed through the super graphics software. Based on analyzed datasets for five various mines, the results and discussion have been described concerning blast-induced ground vibration. This section deals with the proper interpretation and description of measured, predicted, and other associated parameters along with certain correlations by various models.

5.2 Pukka Structures

In this study, several domestic structures were visited and inspected while monitoring ground vibrations in all five various mine and quarry. The wall of pukka houses are made up of sand-cement mortar bricks with or without plaster, and their roofs are made up of customarily reinforced concrete cement and rectangular blocks of rock. The good interconnection or bonding of walls and roof of any structures provide good strength and good sustainability to the ground vibration. However, all the structures continuously accumulate stress energy in the form of strain. This bounded stress-energy tries to release itself along the weakest section of structures cause to damage from cosmetic (hairline) to major. Hairline to minor cracks is developed on plaster walls made of sand cement mortar- bricks structure as shown in Figure 4.7. The cracks developed at the weakest portion of the wall and progressed along the line due to repetitive ground vibration stress. Minor to major cracks was developed at the foundation of the same structure.

5.3 Kuchcha Structures

Visual inspection of the damaged and non-damage structures surrounding mining areas has been carried out. The wall of most structures is made up of clay, mortar, bricks, rocks, and their roof belongs to tin sheet, asbestos sheet, and bamboo and wooden with Kush mesh with a poor foundation. The walls are poorly interconnected and are the main reason for weak strength and poor sustainability of ground vibrations. Minor to major cracks were developed on the clay mortar bricks wall. The cracks developed at the weakest portion of the wall and progressed along the line due to repetitive ground vibration stress. The upper section of the wall becomes a weak zone due to poor bonding, as shown in Figures 4.12 and 4.13. cosmetic (hairline) to minor cracks originate on clay mortar bricks and sand cement mortar bricks with or without plaster structures due to repetitive ground vibration. However, cracks may originate due to environmental factors like temperature, humidity, poor construction materials utilized, and a poor foundation. Random distribution of hairline to minor fractures as shown in Figures 4.10 and 4.11.

5.4 Structural and Human Response to the Ground Vibration

The structure and human response of annoyance due to ground vibration are aggravated by the wall, door, and window rattling. Humans perceive ground vibration at around 0.127mm/sec of peak particle velocity (PPV). The lowest suggested allowable ground vibration for the structures is 1.27mm/sec as unacceptable based on direct reactions to the vibration. The even lower level of ground vibration creates psychological problems. Thus, social and economic issues arise due to repetitively blasting operations. Due to ground vibration, the structures are damaged with hairline, minor and major cracks on with or without plasters walls and roofs.

5.4.1 Case I: Coal mine-1 Chhattisgarh

Structural Response based on USBM RI 8507 model United State Bureau of Mine (USBM) proposed a standard model for blasting damage criteria limits for their local structures close to mine areas based on the PPV with associated dominant frequency. The upper line of the rhombus defines permissible limits of drywall construction, whereas the lower line of the rhombus defines permissible limits of plaster, lath construction. Results have been tabulated in Table 3.2, to which the following conclusions can be drawn.

(i) For monitoring distance of 50m to 200m from blast site at a specific maximum charge per delay of 371kg, frequency vs. amplitude graph plotted on the logarithmic scale for orthogonal radial, transverse, vertical direction as shown in Figures 4.25 to 4.28. From these listed figures, it is evident that the density distribution of spheres is mostly above the permissible limits, and these severely indicate structural damages. The peak particle velocity was obtained as 119.50 mm/s to 20.32 mm/s with the associated dominant frequency of 148Hz to 28.10Hz. The ground vibrations contain high-stress energy in all directions into the surface for moderate to major destruction of any structures at these distances. This may cause damage to the modern homes, drywall interior, older homes, and plaster on wood lath construction structures and should not be safe for such blast event BM_1. Therefore, within 200 m distance from the blast site is the most destructive region.

(ii) For monitoring distance of 250m to 400m from the blast site at a specific maximum charge per delay of 280kg, frequency vs. amplitude graph plotted on the logarithmic scale for orthogonal radial, transverse, vertical direction as shown in Figures 4.29 to 4.32. From these listed figures, it is evident that the density distribution of spheres is mostly below the permissible limits. In contrast, some are above these limits, indicating moderate structural damage. The peak particle velocity was obtained as 11.05 mm/s to 4.82 mm/s with the dominant frequency of 35.20 Hz to 3.80Hz, respectively. The ground vibrations contain enough stress energy for moderate to minor damage to the modern homes, drywall interior, older homes, and plaster on wood lath construction structures. They should not be safe within the distance of 400m and undergo damage for such blast event BM_2. Beyond 350m from the blast site, PPV values become weaker with associated dominant frequency. The region within the distance of 400m may be considered the moderate destructive region.

(iii) For monitoring distance of 450m to 600m from blast site at a specific maximum charge per delay of 324kg for blast event BM_3, frequency vs. amplitude graph plotted on the logarithmic scale of orthogonal radial, transverse, vertical direction as shown in Figures 4.33 to 4.36. From these listed figures, it is evident that the density distribution of spheres is mostly under the permissible limits, and it indicates no instant structural damage. The peak particle velocity was obtained as 6.6 mm/s to 2.54 mm/s with the associated dominant frequency of 8.0Hz to 2.80Hz, respectively. The ground vibrations contain enough stress-energy, which damages moderate to minor due to the repetitively of ground vibration for a long period to modern homes, drywall interior, older homes, and plaster on wood lath construction structures. Within 600m, PPV becomes weaker with associated dominant frequency at which all structures should be safe for a short period and considered a semi-moderated destructive region.

(iv) For the monitoring distance of 650m to 800m from the blast site at a specific maximum charge per delay of 475kg for blast event BM_4, frequency vs. amplitude graph plotted on the logarithmic scale for orthogonal radial, transverse, vertical direction as shown in Figures 4.37 to 4.40. From these listed figures, it is evident that the density distribution of spheres is much lower under the permissible limits, and it indicates minor to threshold structural damage due to repetitively ground vibration. The peak particle velocity was obtained as 3.17 mm/s to 1.56 mm/s with the associated dominant frequency of 24.7Hz to 28.0Hz, respectively. The ground vibration contains much weaker stress energy that causes damages minor to the cosmetic (hairline) to modern homes, drywall interior, older homes, and plaster on wood lath construction structures. Within the distance of 650m, PPV becomes much weaker with associated dominant frequency at which all structures should be safe for a longer period of time. The structures present in this region are considered to be minor destructive regions.

(v) For the monitoring distances of 900m to 950m from the blast site at a specific maximum charge per delay of 470kg for blast event BM_5, frequency vs. amplitude graph plotted on the logarithmic scale for orthogonal radial, transverse, vertical direction as shown in Figures 4.41 and 4.42. From these listed figures, it is evident that the density distribution of spheres is much lower under the permissible limits, and it indicates threshold structural damage due to repetitively ground vibration. The peak particle velocity was obtained as 3.05 mm/s to 2.16 mm/s with the associated dominant frequency of 6.3Hz and 13.9Hz, respectively. Again, the ground vibration contains much weaker stress-energy and is not enough for immediate damages to modern homes, drywall interior, older homes, and plaster on wood lath construction structures. Beyond the distance of 1000m, PPV becomes much weaker and weaker with associated dominant frequency at which all structures should be safe for a much longer period of time. The structures present in this region are considered threshold destructive regions.

The results and discussion based on Indian standard, DGMS circular no. 7 of 1997 for proposed damage criteria as a structural response to the domestic, industrial, and objects of historical importance and sensitive structures are given here. Different structures indicate continuous red line, blue brake line, and black dotted line for the domestic houses (kuchcha and pukka), industrial building, and objects of historical importance and sensitive structures, respectively, on the logarithmic scale graph. The historical importance structures were not present in the study area; however domestic houses and industrial structures were present at a nearby mine. The results have been tabulated in Table 3.2, by which the following conclusions can be drawn.

(i) For monitoring distance of 50m to 200m from blast site at a specific maximum charge per delay of 371kg, frequency vs. amplitude graph plotted on the logarithmic scale for orthogonal radial, transverse, vertical direction as shown in Figures 4.43 to 4.46. From these listed figures, it is evident that the density distribution of spheres is mostly above the permissible limits, which severely indicates structural damage. The peak particle velocity was obtained as 119.50 mm/s to 20.32 mm/s with the associated dominant frequency of 148Hz to 28.10Hz. The ground vibrations contain high-stress energy in all directions into the surface for moderate to major destruction of any type of structures at these distances. This may cause damage to all the structures such as domestic, industrial, and objects of historical importance, and sensitive structures should not be safe for such blast event BM_1. Therefore, the severely destructive region is within 200 m from the blast site.

(ii) For monitoring distance of 250m to 400m from the blast site at a specific maximum charge per delay of 280kg, frequency vs. amplitude graph plotted on the logarithmic scale for orthogonal radial, transverse, vertical direction as shown in Figures 4.47 to 4.50. From these listed figures, it is evident that the density distribution of spheres is mostly below the permissible limits, whereas some are above these limits, and it indicates moderate structural damage. The peak particle velocity was obtained as 11.05 mm/s to 4.82 mm/s with the dominant frequency 35.20 Hz to 3.80Hz, respectively. The ground vibrations contain enough stress energy for moderate to minor damage to all the structures such as domestic, industrial, and objects of historical importance and sensitive structures. They should not be safe within the distance of 400m and undergoes instant damage to the historical importance and sensitive structures for the blast event BM_2. Beyond 400m from the blast site, PPV becomes weaker with associated dominant frequency. The region within the distance of 400m may be considered the moderate destructive region for domestic and industrial, while the severe destructive region for objects of historical importance and sensitive structures.

(iii) For monitoring distance of 450m to 600m from blast site at a specific maximum charge per delay of 324kg for blast event BM_3, frequency vs. amplitude graph plotted on the logarithmic scale of orthogonal radial, transverse, vertical direction as shown in Figures 4.51 to 4.54. From these listed figures, it is evident that the density distribution of spheres is mostly under the permissible limits, and it indicates no instant structural damage. The peak particle velocity was obtained as 6.6 mm/s to 2.54 mm/s with the associated dominant frequency of 8.0Hz to 2.80Hz, respectively. The ground vibration contains enough stress energy from moderate to minor long durational destruction due to repetitive ground vibrations to the domestic, industrial, and objects of historical importance and sensitive structures. Beyond 600m, PPV becomes weaker with associated dominant frequency. The industrial structures present within this region should be safe, while the domestic and objects of historical importance and sensitive structures may not be safe for a longer period of time. This region may be considered as a semi moderate destructive region.

(iv) For the monitoring distance of 650m to 800m from the blast site at a specific maximum charge per delay of 475kg for blast event BM_4, frequency vs. amplitude graph plotted on the logarithmic scale for orthogonal radial, transverse, vertical direction as shown in Figures 4.55 to 4.58. From these listed figures, it is evident that the density distribution of spheres is much lower under the permissible limits, and it indicates minor to threshold structural damage due to repetitive ground vibrations. The peak particle velocity was obtained as 3.17 mm/s to 1.56 mm/s with the associated dominant frequency of 24.7Hz to 28.0Hz, respectively. The ground vibration contains weaker stress energy and is responsible for minor to hairline damages due to the repetition of ground vibration to the domestic and sensitive structures for a longer period of time. Beyond the distance of 800m, PPV becomes much weaker with associated dominant frequency. Industrial and domestic structures should be safe within this region, while sensitive structures may not be safe for a longer time. The structures present in this region are considered to be minor destructive regions.

(v) For the monitoring distances of 900m to 950m from the blast site at a specific maximum charge per delay of 470kg for blast event BM_5, frequency vs. amplitude graph plotted on the logarithmic scale for orthogonal radial, transverse, vertical direction as shown in Figures 4.59 and 4.60. From these listed figures, it is evident that the density distribution of all spheres is much lower under the permissible limits, and it indicates threshold structural damage due to repetitive ground vibrations. The peak particle velocity was obtained as 3.05 mm/s to 2.16 mm/s with the associated dominant frequency 6.3Hz and 13.9Hz, respectively. The ground vibration is again much weaker and not enough for any instant damages to all types of structures. Beyond the distance of 1000m, PPV values become much weaker and weaker with associated dominant frequency at which all the structures should be safe for a much longer time. The structures present in this region are considered threshold destructive regions.

5.4.1.1 Conventional Approach

To establish the relationship (5.1) among monitoring distance, the maximum charge per delay, and PPV for a particular mine dataset of Table 3.3 and predict PPV values. Where the value of k =176.03 and b = -1.626 are site characteristics constants. Site constants depend on the physical properties of the rock mass. They can change from one site to another site. They can find out through simple linear regression analysis.

$$PPV = 176.03 * (D^{2/3}/Q)^{-1.626} \quad (5.1)$$

Linear regression analysis is used to determine the site characteristics constant of rock mass, and site constant varies from one site to another the site due to changes in physical properties of the rock mass. Derived an equation among relation measured peak particle velocity, monitoring distance, and maximum charge per delay and obtained the predicted PPV. Scaled distance is the function of monitoring distance and maximum charge per delay, and obtained correlation coefficient between measured peak particle velocity and scaled distance is 83%, as shown in Figure 5.1. whereas, between monitoring distance and measured PPV is around 57.59%, as shown in Figure 5.2. The main objective is to determine a better correlation coefficient between measured and predicted peak particle velocity of 72.90%, as shown in Figure 5.3. This supports computational study against minefield at minimum cost and optimizes blast design parameters.

5.4.1.2 Multivariate Regression Analysis Approach

In the ongoing study, the multivariate regression analysis (MVRA) applied nine independent variables instead of two variables (conventional approaches) to predict PPV and frequency and gave enhanced and significant correlation. Established the relationship for the PPV and frequency with various parameters are given in equations (5.2 and 5.3). The significant correlation coefficient between measured and predicted peak particle velocity is 75.76%, shown in Figure 5.4. However, the correlation coefficient between monitoring and measured peak particle velocity is 65.0%, and the correlation between measured and predicted frequency is 26% are shown in Figures 5.5 and 5.6, respectively.

PPV = 30.17128-0.0097*D+0.05942*MCPD+0.0014144*TC+0.826352*TB+ 2.227614*B - 0.72062*S-0.37704*NH-5.00792*HD+0.066992*HDI (5.2)

Frequency(f)=6.54903-0.02968*D-0.02345*MCPD+0.00719*TC-0.15732*TB-47.2639*B+29.25495*S+0.534418*NH+15.3229*HD-0.26691*HDI (5.3)

Where D- Distance (m), MCPD- Maximum charge per delay (kg), TC- Total Charge (kg), TB-Total Booster (kg), B- Burden(m), S- Spacing (m), NH- No. of Holes (cont.), HD- Depth of hole (m), HDI-Diameter of the hole (mm).

5.4.1.3 Backpropagation artificial neural network approach

The backpropagation ANN approach is used for various datasets to make an easy computational study to predict and analyze blast-induced ground vibration parameters like PPV and frequency. In the ongoing study, the backpropagation artificial neural network BPANN approach has applied nine independent variables parameters like multivariate regression analysis to predict PPV and frequency. The backpropagation ANN approach enhanced the correlation coefficient over MVRA and other models. The correlation coefficient between monitoring distance and measured PPV is 71.76%, as shown in Figure 5.7. However, the correlation coefficient between measured and predicted PPV and frequency are 92.04% and 60.65%, which are shown in Figures 5.8 and 5.9, respectively. The main emphasis of this study is to establish a better correlation coefficient between the measured and predicted values. All models are applicable to optimizing blast design parameters to reduce the intensity of ground vibrations and safe and smooth blasting operation. The wavelets of measured and predicted IS, MVRA, and ANN obtained PPV, and varying with datasets is combined in Figure 5.10. MVRA and ANN obtained the wavelets of measured and predicted frequency, varying with datasets as shown in Figure 5.11. The derived equation for PPV and frequency as given in Equations 5.4 and 5.5, respectively.

PPV = 29.17128 0.0097*D+0.06342*MCPD+0.003244*TC+ 0.96554*TB + 4.147517*B - 0.87758*S-0.47822*NH-9.2458*HD +0.024587*HDI (5.4)

Frequency (f)= 12.36803- 0.12897*D-0.03694*MCPD+0.006971*TC-0.26974*TB-34.4572*B +49.4678*S+0.768954*NH +19.5234*HD-0.78341*HDI (5.5)

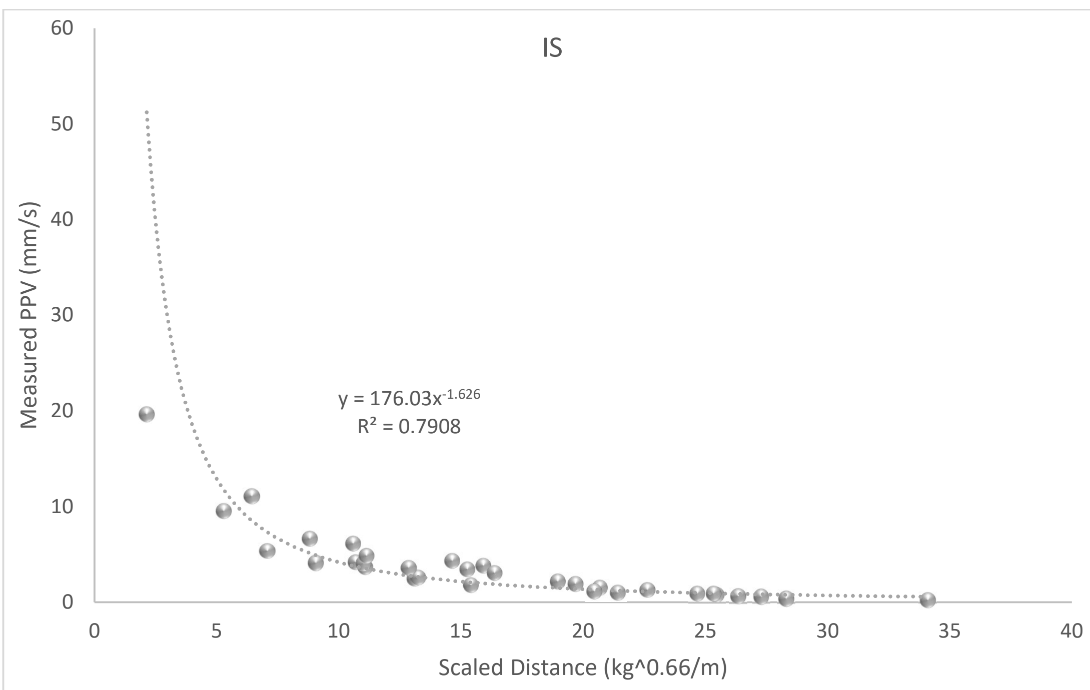

Figure 5.1 Scattered plots between scaled distance and measured PPV by IS.

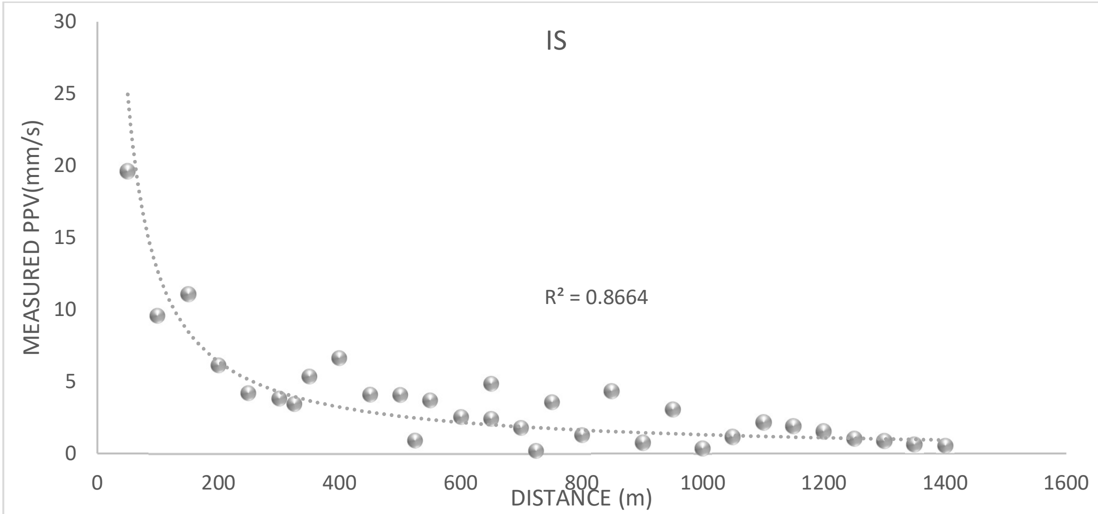

Figure 5.2 Scattered plots between distance and measured PPV by IS.

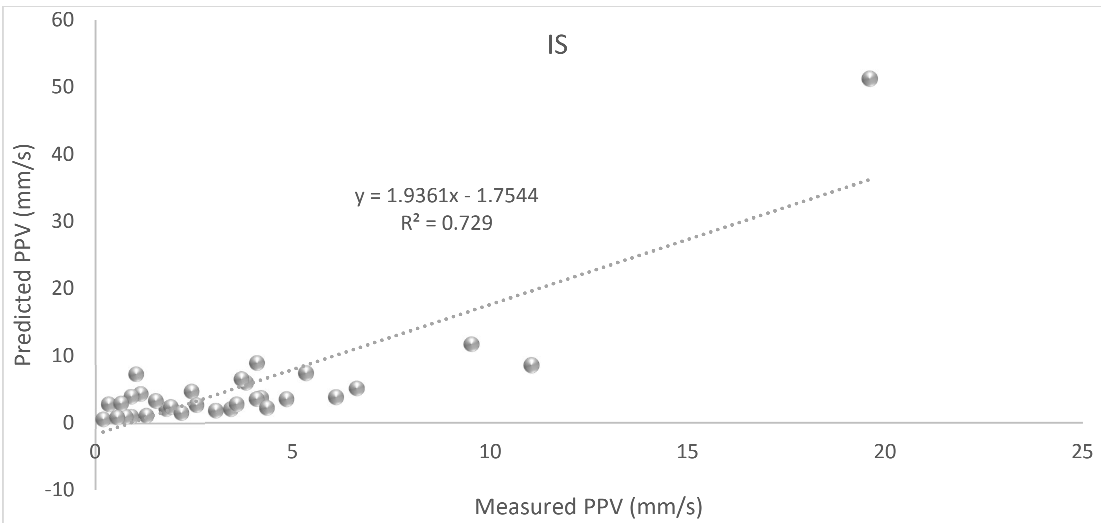

Figure 5.3 Scattered plots between measured and predicted PPV by IS.

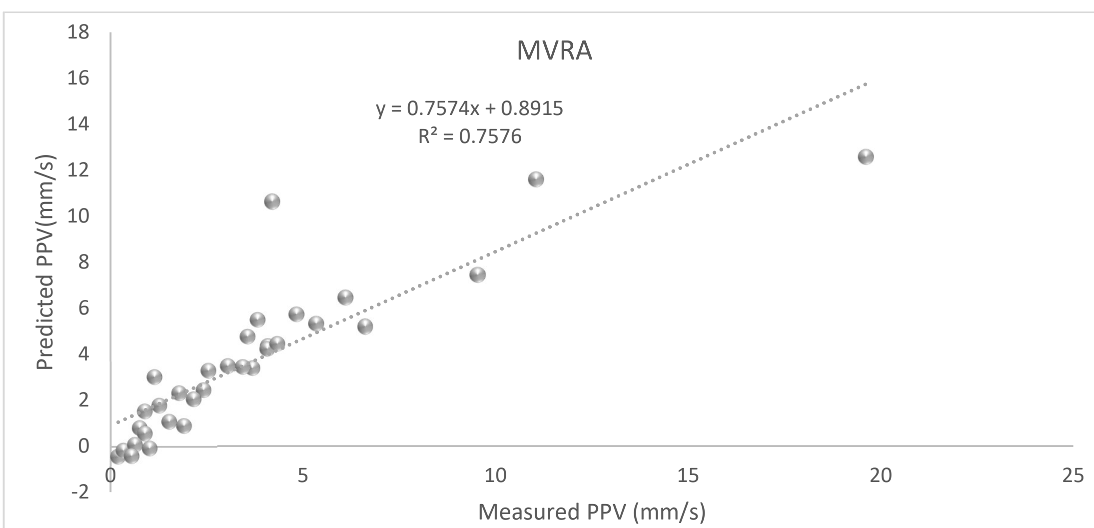

Figure 5.4 Scattered plots between measured and predicted PPV by MVRA.

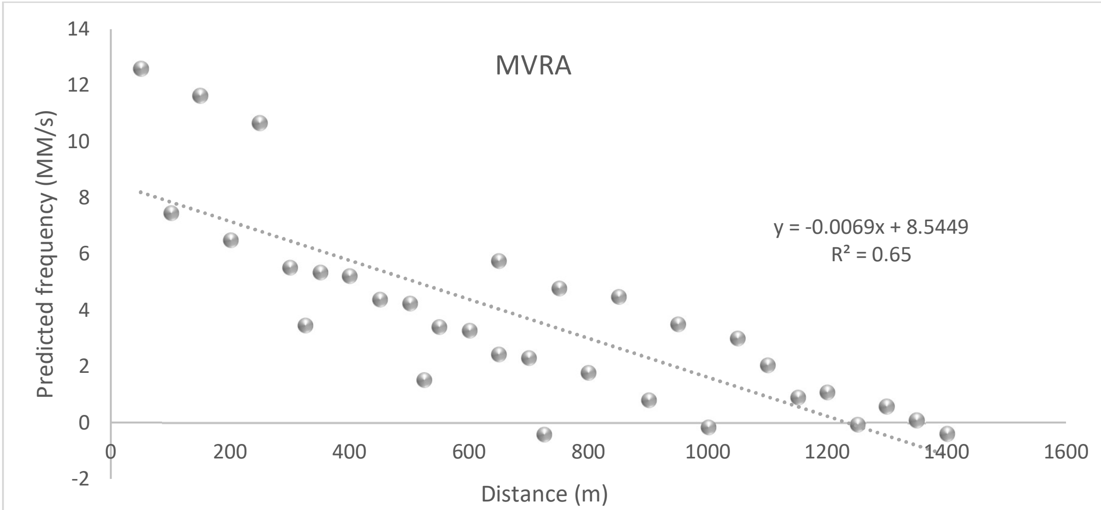

Figure 5.5 Scattered plots between distance and predicted frequency by MVRA.

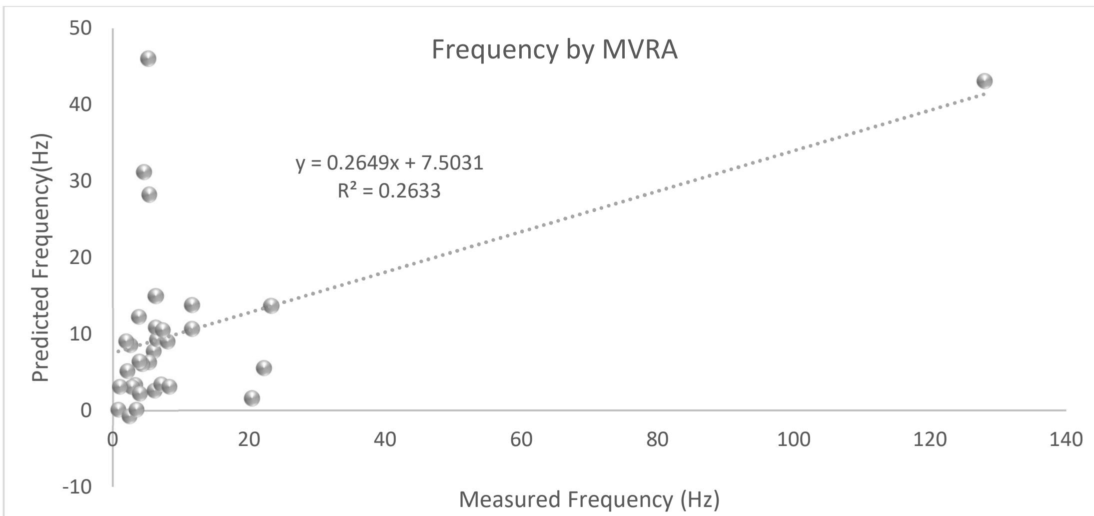

Figure 5.6 Scattered plots between measured and predicted frequency by MVRA.

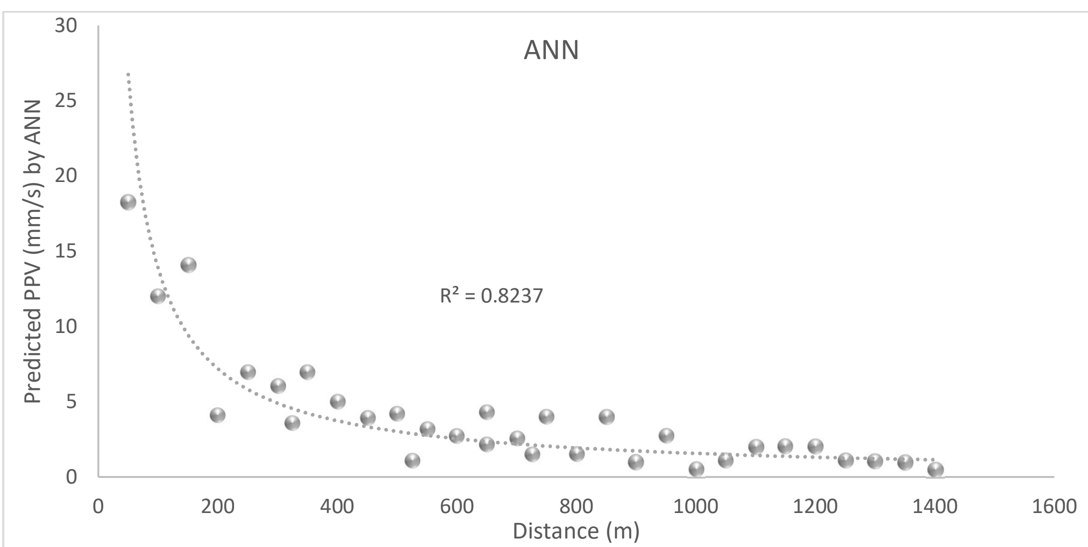

Figure 5.7 Scattered plots between distance and predicted PPV by ANN.

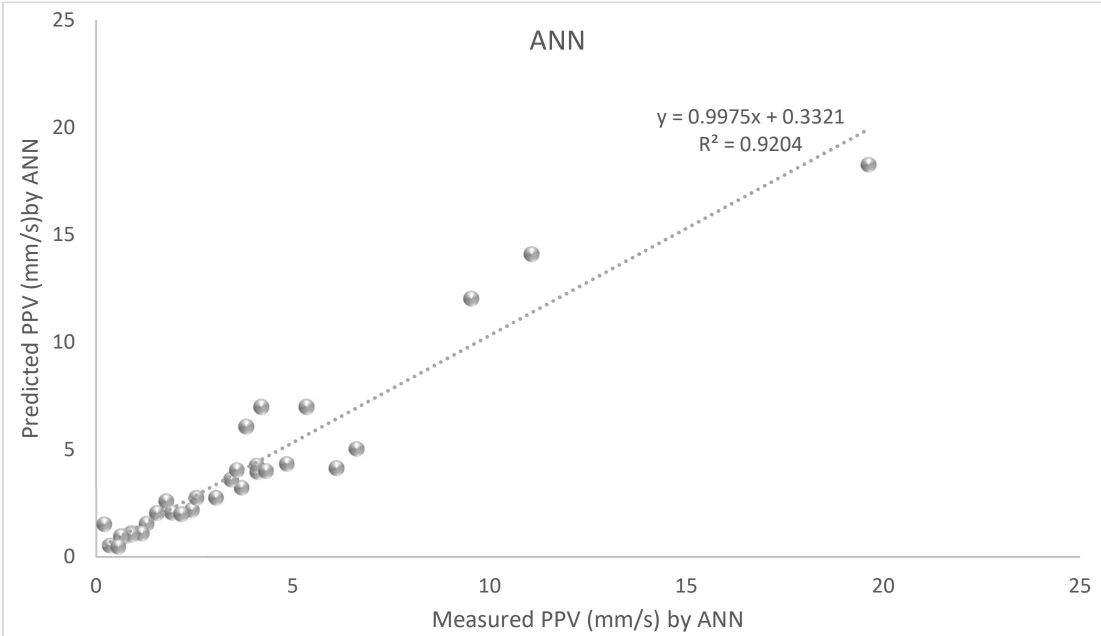

Figure 5.8 Scattered plots between measured and predicted PPV by ANN.

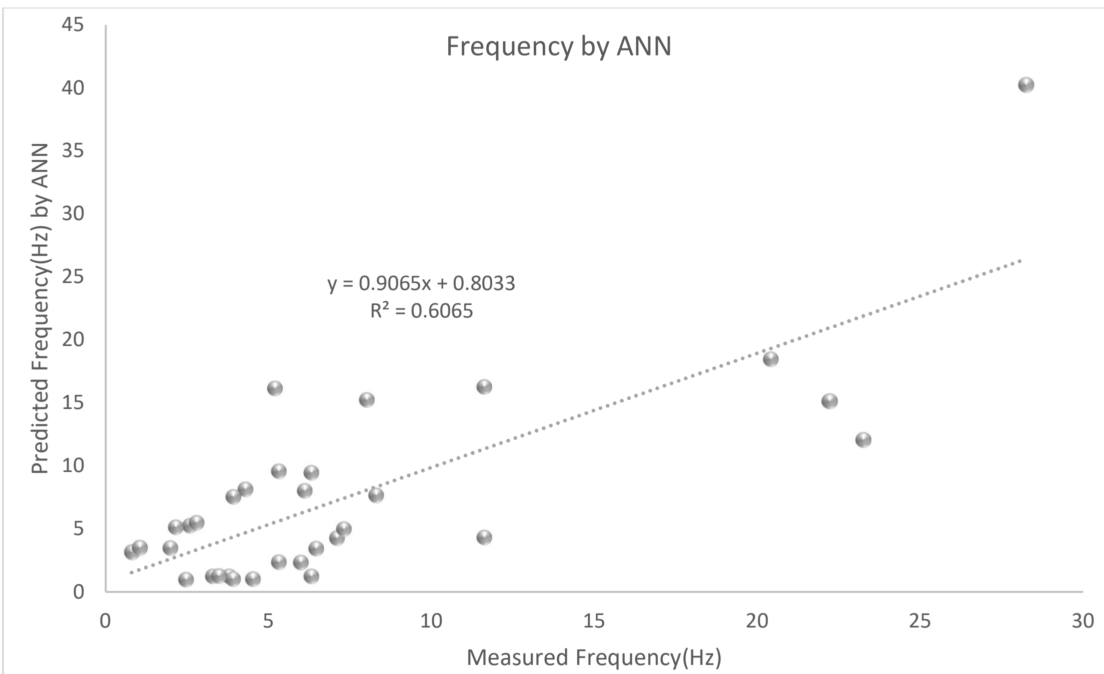

Figure 5.9 Scattered plots between measured and predicted frequency by ANN.

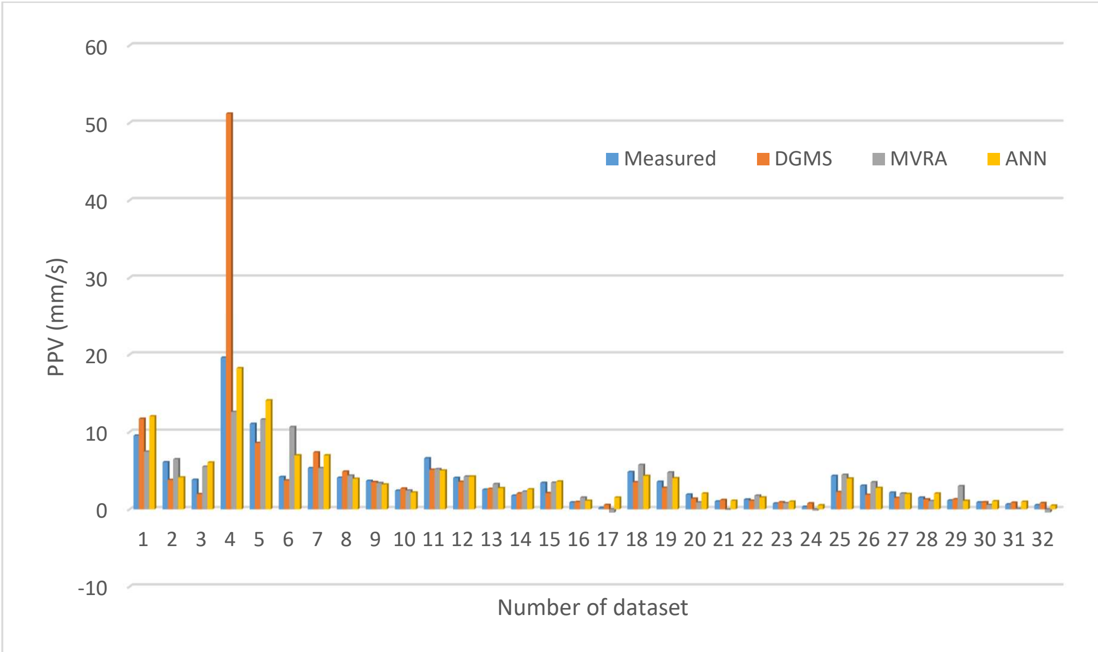

Figure 5.10 Measured and predicted PPV with datasets.

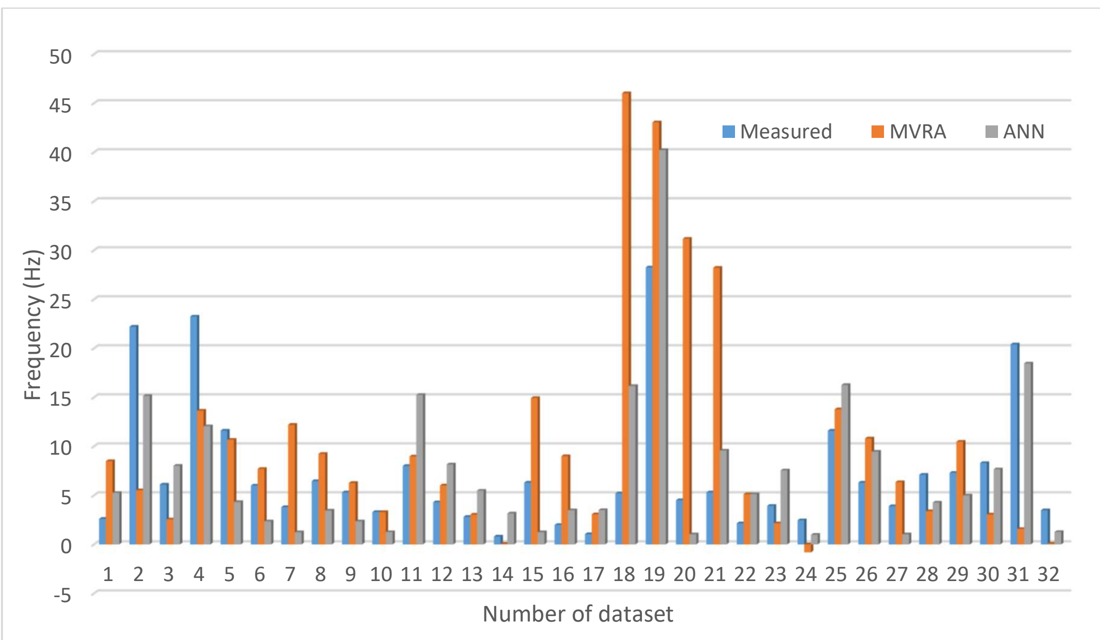

Figure 5.11 Measured and predicted frequency with datasets.

5.4.1.4 Safe Charge per Delay

In the ongoing discussion, the main objective is to find a safe charge for domestic structures like kuchcha and pukka houses near the mine site. The Indian standard proposed permissible limits for the domestic structure is 5mm/s of peak particle velocity at a frequency less than 8 Hz. It may be used to prevent damage to structures surrounding the mine site. Consideration of permissible limit of peak particle velocity is 5mm/s, and monitoring distance from the blast site enables to derive the expression for the calculation of safe charge weight per delay or maximum charge per delay is given in Equation (5.6) using the data tabulated in Table 3.4. Table 5.1 shows the safe charge weight per delay with a varying distance of 100m interval. The distribution of maximum charge per delay with safe distances is shown in Figure 5.12.

$$Q_{max} = D^{0.66} * (PPV/0.726)^{0.8045} \quad (5.6)$$

Table 5.1: The safe charge weight per delay distribution

Distance (m)	Safe Charge Weight per Delay (kg)	Distance (m)	Safe Charge Weight per Delay (kg)
200	155.91	1200	508.69
300	203.75	1300	536.29
400	246.35	1400	563.17
500	285.44	1500	589.41
600	321.94	1600	615.05
700	356.42	1700	640.16
800	389.25	1800	664.77
900	420.72	1900	688.93
1000	451.02	2000	712.65
1100	480.30	2100	735.97

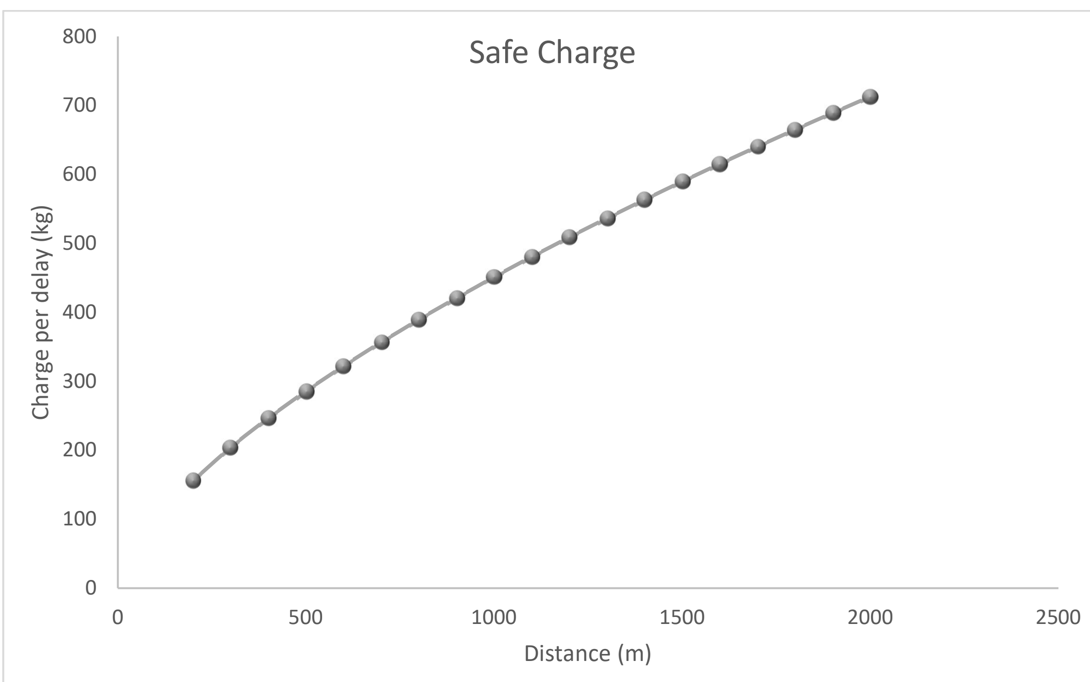

Figure 5.12 Safe charge weight per delay distribution.

5.4.1.5 Critical Distance Assumption

The monitoring distance and the maximum charge per delay are vital in predicting the BIGV vis-à-vis the safety of structures near the mine site. In the ongoing discussion, the critical distance is proposed as 300–550 m from the blast site at the maximum charge per delay of 475 kg. On measuring the intensity of BIGV at the above distances, the structures were safe at the maximum charge per delay of 475 kg. According to the Indian Standard provided by DGMS, the domestic structures should be safe within 5mm/s at <8 Hz. The peak particle velocity observed within 300 m from the blast site was higher at the maximum charge per delay. The permissible limit for the different types of structures is accessed as a black dotted line for the sensitive structures, a continuous red line for the domestic structures, and a blue break line for the industrial structures. From figures 5.13 and 5.14, the density of spherical bubbles lies above the black dotted line and below the red continuous. This implies that only the sensitive structures should be damaged; however, domestic and industrial structures should be safe. From figures 5.15 and 5.16, the peak particle velocity is observed less than 4.5 mm/s at a dominant frequency of less than 10 Hz depicts that only the sensitive structures may undergo damage. At the same time, domestic and industrial buildings should be safe.

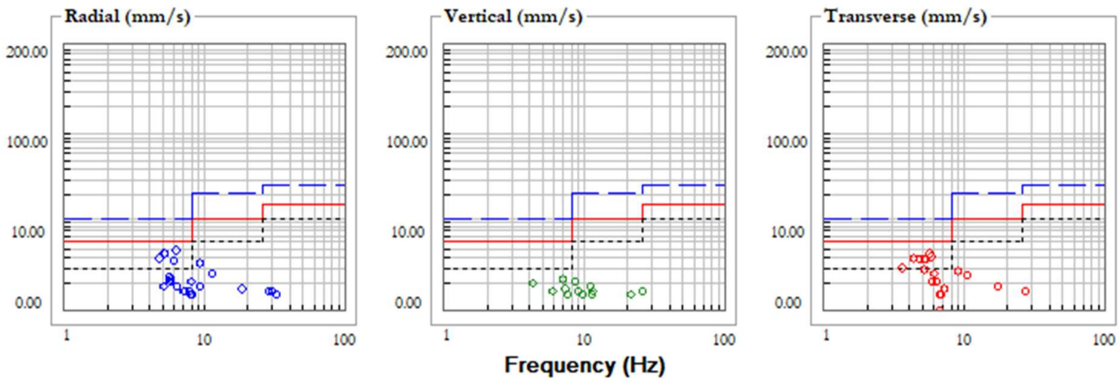

Figure 5.13 blast event at monitoring distance of 300m

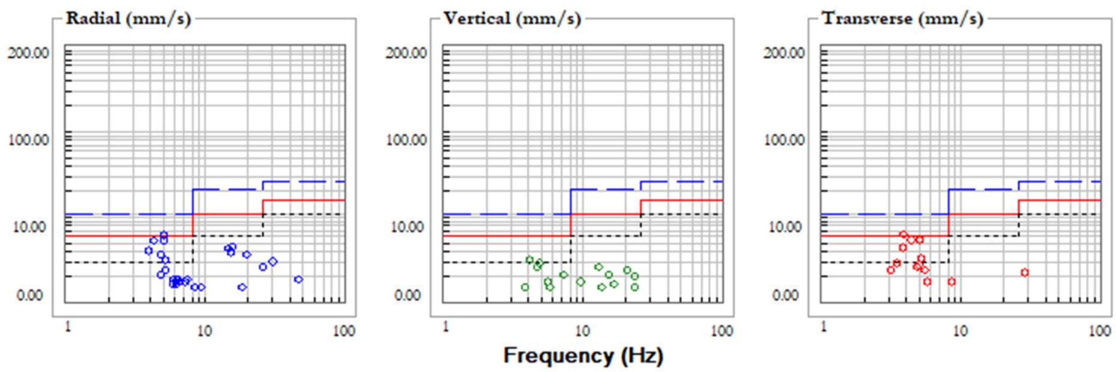

Figure 5.14 blast event at monitoring distance of 350m

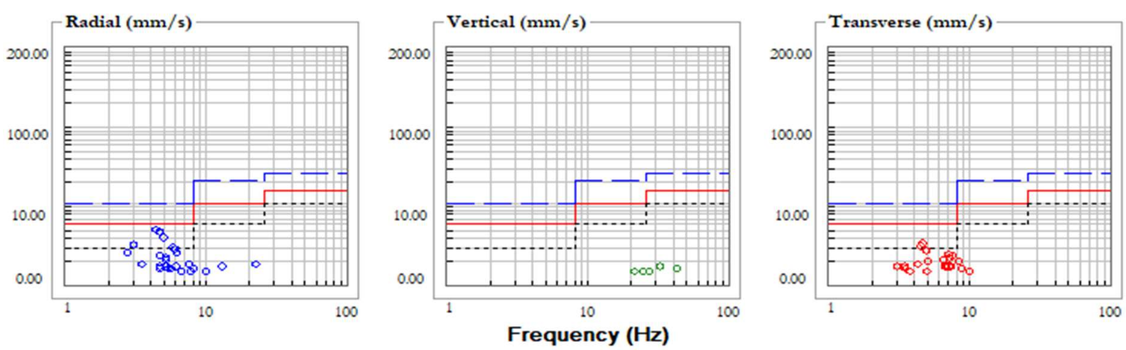

Figure 5.15 blast event at monitoring distance of 500m

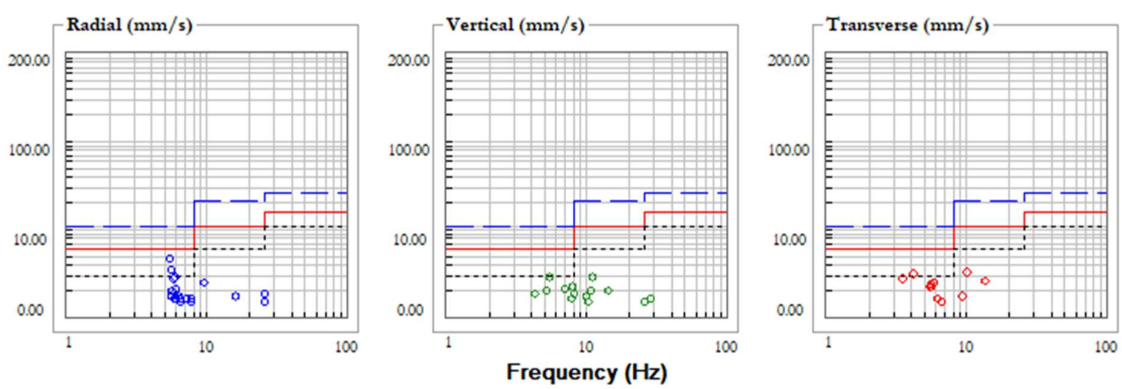

Figure 5.16 blast event at monitoring distance of 550m.

5.4.1.6 Peak Particle Velocity Assumption

A seismograph records the radial, transverse and vertical velocities. These velocities are analyzed on the computer by using super graphic software. It helps pick the maximum amplitude among the three velocities to define the peak particle velocity. The wavelet's first, second, and third breaks are defined as the P-wave, S-wave, and surface wave, respectively. The surface wave has a maximum amplitude and causes more damage than the other two waves. PPV is purely a surface wave. By regression analysis, a correlation has been generated between component velocities like radial, transverse, and vertical with measured PPV. The correlation coefficient among the velocity components in orthogonal like radial, transverse and vertical direction are 98.37%, 98.34%, and 89.34%, respectively, as shown in Figure 5.17. The radial and transverse velocity components give a better correlation with measured PPV than the vertical component.

5.4.1.7 Correlation

The correlation coefficient between monitoring distance and peak particle velocity is 49.26% and 25.61%, respectively, as shown in Figure 5.18. The correlation coefficient between scaled distance and peak particle velocity is 63.94%, 31.28% shown in Figure 5.19. The correlation coefficients for radial velocity is 49.93%, transverse velocity is 44.10%, and vertical velocity is 35.66% with monitoring distance, as shown in Figure 5.20. The correlation coefficient obtained for radial velocity is 62.28%, transverse velocity is 75.20%, and vertical velocity is 46.68% with scaled distance, as shown in Figure 5.21. The correlation coefficient between frequency and peak particle velocity is 62.67%, as shown in Figure 5.22.

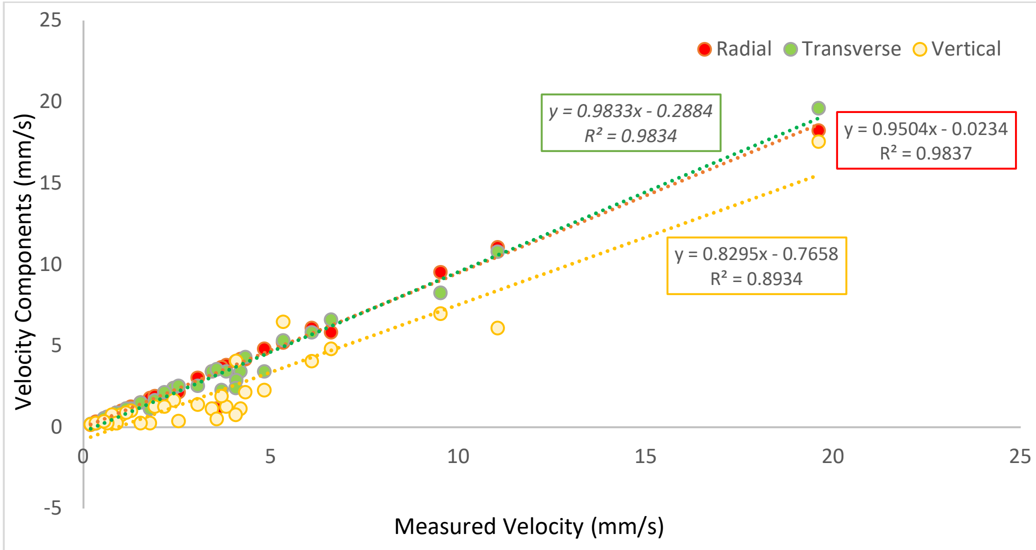

Figure 5.17 Correlation of component velocities with principal velocity

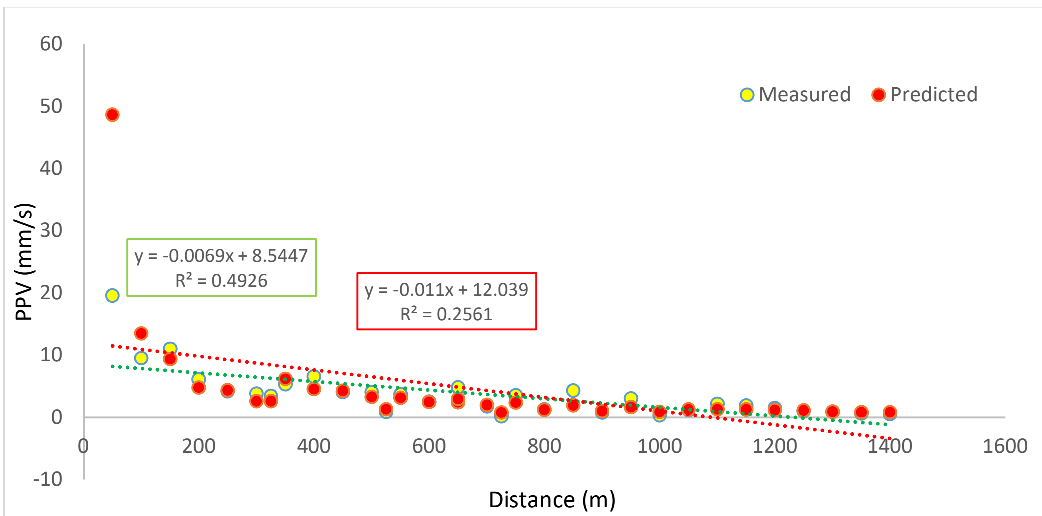

Figure 5.18 Graph plotted of measured and predicted PPV with monitoring distance.

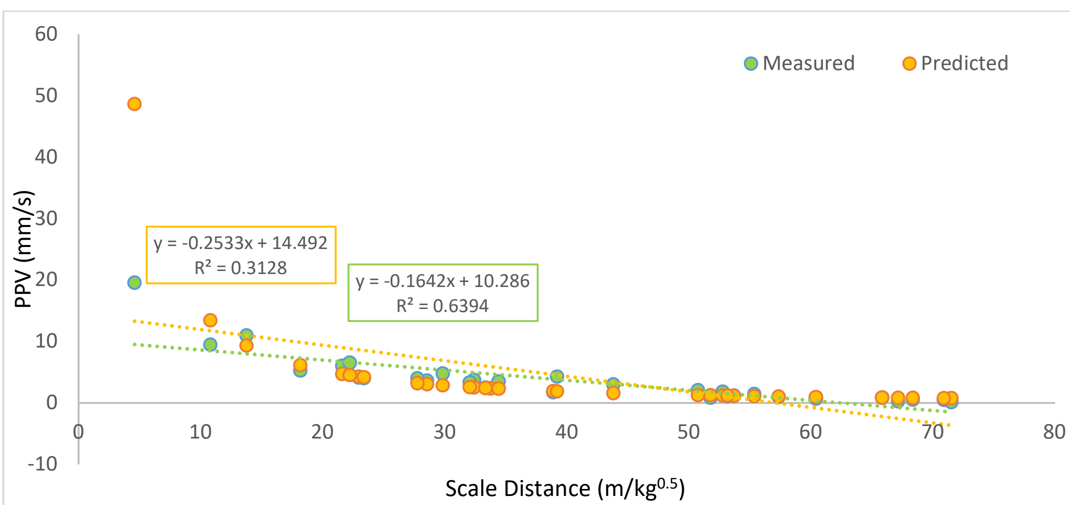

Figure 5.19 Graph plotted of measured and predicted PPV with Scaled distance.

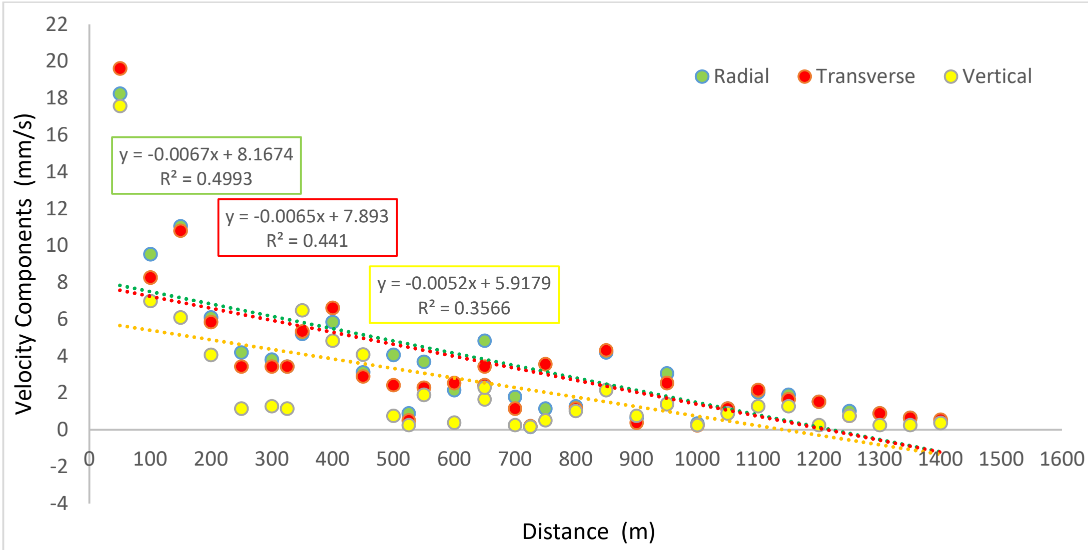

Figure 5.20 Graph plotted of velocity components with monitoring distance.

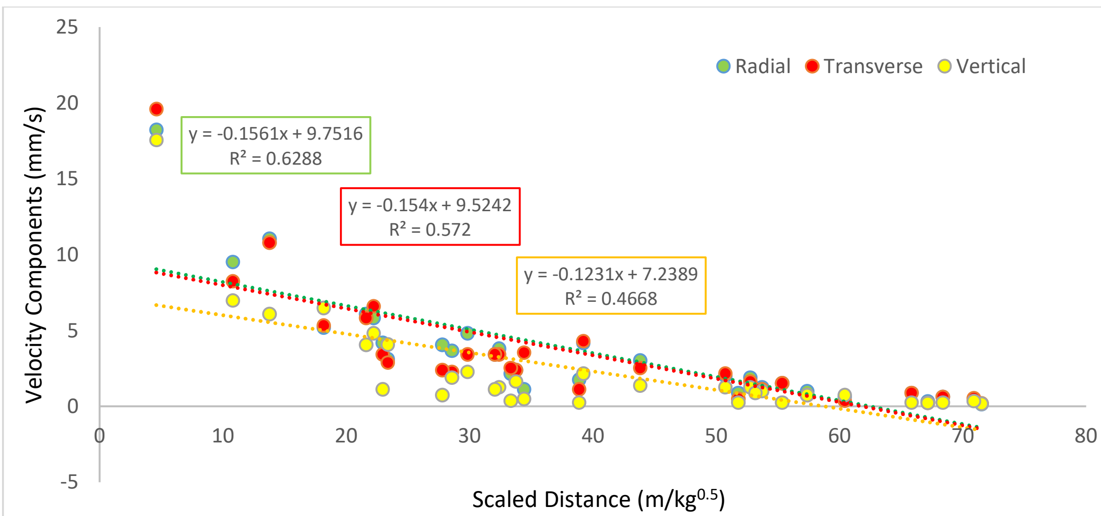

Figure 5.21 Graph plotted of velocity components with scaled distance.

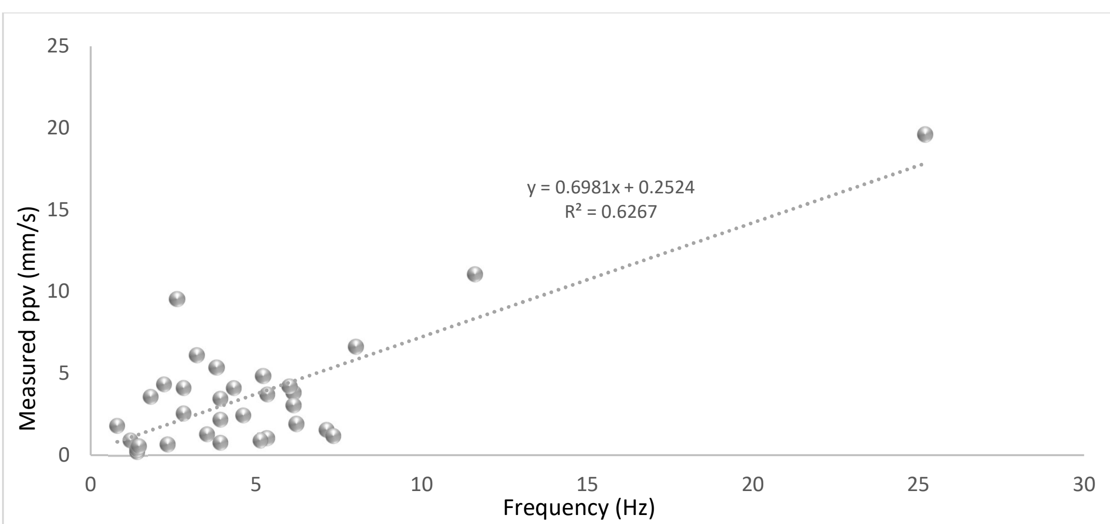

Figure 5.22 Graph plotted between measured peak particle velocity and measured frequency.

5.4.2 Case II: Coal mine-2 Madhya Pradesh

The following conclusions can be drawn based on Table 3.8 for opencast coal mine-2.

(i) For monitoring distance of 50m to 200m from blast site at a specific maximum charge per delay of 950kg, frequency vs. amplitude graph plotted on the logarithmic scale for orthogonal radial, transverse, vertical direction as shown in Figures 4.62 to 4.65. From these listed figures, it is evident that the density distribution of spheres is mostly above the permissible limits, which severely indicates structural damage. The peak particle velocity was obtained as 91.57 mm/s to 9.73 mm/s, with the associated dominant frequency of 5.5Hz to 9.8Hz. The ground vibrations contain high-stress energy in all directions into the surface for moderate to major destruction of any type of structures at these distances. This may cause damage to all the structures such as domestic, industrial, and objects of historical importance, and sensitive structures should not be safe for such blast event BEN_1. Therefore, the severely destructive region is within 200 m from the blast site.

(ii) For monitoring distance of 250m to 400m from the blast site at a specific maximum charge per delay of 645kg, frequency vs. amplitude graph plotted on the logarithmic scale for orthogonal radial, transverse, vertical direction as shown in Figures 4.66 to 4.69. From these listed figures, it is evident that the density distribution of spheres is mostly below the permissible limits. In contrast, some are above these limits, and it indicates moderate structural damage. The peak particle velocity was obtained as 7.62 mm/s to 4.70 mm/s with the dominant frequency of 3.6Hz to 5.8Hz, respectively. The ground vibrations contain enough stress energy for moderate to minor damage to all the structures such as domestic, industrial, and objects of historical importance and sensitive structures and should not be safe within the distance of 400m and undergoes instant damage to the historical importance and sensitive structures for the blast event BEN_2. Beyond 400m from the blast site, PPV becomes weaker with associated dominant frequency. The region within 400m may be considered the moderate destructive region for domestic and industrial, while the severe destructive region for objects of historical importance and sensitive structures.

(iii) For monitoring distance of 450m to 600m from blast site at a specific maximum charge per delay of 704kg for blast event BEN_3, frequency vs. amplitude graph plotted on the logarithmic scale of orthogonal radial, transverse, vertical direction as shown in Figures 4.70 to 4.73. From these listed figures, it is evident that the density distribution of spheres is mostly under the permissible limits, and it indicates no instant structural damage. The peak particle velocity was obtained as 6.2mm/s to 3.30mm/s with the associated dominant frequency as 17.6Hz to 12.4Hz, respectively. The ground vibrations contain enough stress energy for moderate to minor long durational destruction due to repetitive ground vibration on domestic, industrial, and objects of historical importance and sensitive structures. Beyond 600m, PPV becomes weaker with associated dominant frequency. The industrial structures present within this region should be safe. In contrast, the domestic and objects of historical importance and sensitive structures may not be safe for a longer period of time. This region may be considered as a semi moderate destructive region.

(iv) For the monitoring distance of 650m to 800m from the blast site at a specific maximum charge per delay of 540kg for blast event BEN_4, frequency vs. amplitude graph plotted on the logarithmic scale for orthogonal radial, transverse, vertical direction as shown in Figures 4.74 to 4.77. From these listed figures, it is evident that the density distribution of spheres is much lower under the permissible limits, and it indicates minor to threshold structural damage due to repetitively ground vibration. The peak particle velocity was obtained as 2.92mm/s to 1.20mm/s with the associated dominant frequency of 36.5Hz to 83.5Hz, respectively. The ground vibration contains weaker stress energy and is responsible for minor to hairline damages due to the repetition of ground vibration to the domestic and sensitive structures for a longer period of time. Beyond the distance of 800m, PPV becomes much weaker with associated dominant frequency. Industrial and domestic structures should be safe within this region, while sensitive structures may not be safe for a longer time. The structures present in this region are considered to be minor destructive regions.

(v) For the monitoring distance of 850m to 1000m from the blast site at a specific maximum charge per delay of 470kg for blast event BM_5, frequency vs. amplitude graph plotted on the logarithmic scale for orthogonal radial, transverse, vertical direction as shown in Figures 4.78 and 4.85. From these listed figures, it is evident that the density distribution of all spheres is much lower under the permissible limits, and it indicates threshold structural damage due to repetitively ground vibration. The peak particle velocity was obtained as 2.28 mm/s to 1.02 mm/s with the associated dominant frequency of 9.1Hz and 12.8Hz, respectively. The ground vibration is again much weaker and not enough for any instant damages to all types of structures. Beyond the distance of 1000m, PPV values become much weaker and weaker with associated dominant frequency at which all the structures should be safe for a much longer time. The structures present in this region are considered threshold destructive regions.

5.4.2.1 Safe Charge Weight per Delay

In the ongoing discussion, the main objective is to find a safe charge for domestic structures like kuchcha and pukka houses near the mine site. The Indian standard proposed permissible limits for the domestic structure is 5mm/s of peak particle velocity at a frequency less than 8 Hz. It may be used to prevent damage to structures surrounding the mine site. Consideration of permissible limit of peak particle velocity is 5mm/s, and monitoring distance from the blast site enables to derive the expression for the calculation of safe charge weight per delay or maximum charge per delay equations are tabulated in Table 5.2 using the data tabulated in Table 3.9. Table 5.3 shows safe charge weight per delay with a varying distance of 50m interval. The distribution of maximum charge per delay with safe distances, as shown in Figure 5.23.

Table 5.2: Safe charge weight per delay formulae

Sl. No.	References	Equations
1	Duvall-Petkof D-P (1959)	$Q_{max}= D^{2}*(PPV/k)^{2/b}$
2	Langefors-Kihlstrom L-K (1963)	$Q_{max}= D^{0.66}*(PPV/k)^{2/b}$
3	General predictor GP (1964)	$Q_{max}= D^{b/a} *(PPV/k)^{1/a}$
4	Ambraseys-Hendron A-H (1968)	$Q_{max}= D^{3}*(PPV/k)^{3/b}$
5	Indian Standard IS (1973)	$Q_{max}= D^{0.66}*(PPV/k)^{-1/b}$

Table 5.3: Obtained safe charge weight per delay using the above formulae

Monitoring Distance (m)	Safe Charge Weight by D-P (kg)	Safe Charge Weight by L-K (kg)	Safe Charge Weight by GP (kg)	Safe Charge Weight by A-H (kg)	Safe Charge Weight by IS (kg)
200	194.14	537.10	180.68	99.48	545.30
250	303.35	622.32	287.32	194.31	631.82
300	436.82	701.90	419.72	335.77	712.62
350	594.56	777.07	578.2	533.20	788.94
400	776.57	848.66	763.25	795.91	861.62
450	982.85	917.26	974.99	1133.24	931.27
500	1213.4	983.32	1213.71	1554.52	998.34
550	1468.22	1047.16	1479.6	2069.06	1063.16
600	1747.303	1109.06	1773.01	2686.21	1126.0
650	2050.65	1169.22	2093.97	3415.28	1187.08
700	2378.27	1227.83	2442.72	4265.60	1246.59
750	2730.16	1285.04	2819.41	5246.50	1304.66
800	3106.31	1340.95	3224.20	6367.31	1361.44
850	3506.73	1395.70	3657.22	7637.35	1417.02
900	3931.43	1449.36	4118.63	9065.96	1471.49
950	4380.39	1502.01	4608.53	10662.45	1524.95
1000	4853.61	1553.73	5127.06	12436.16	1577.46

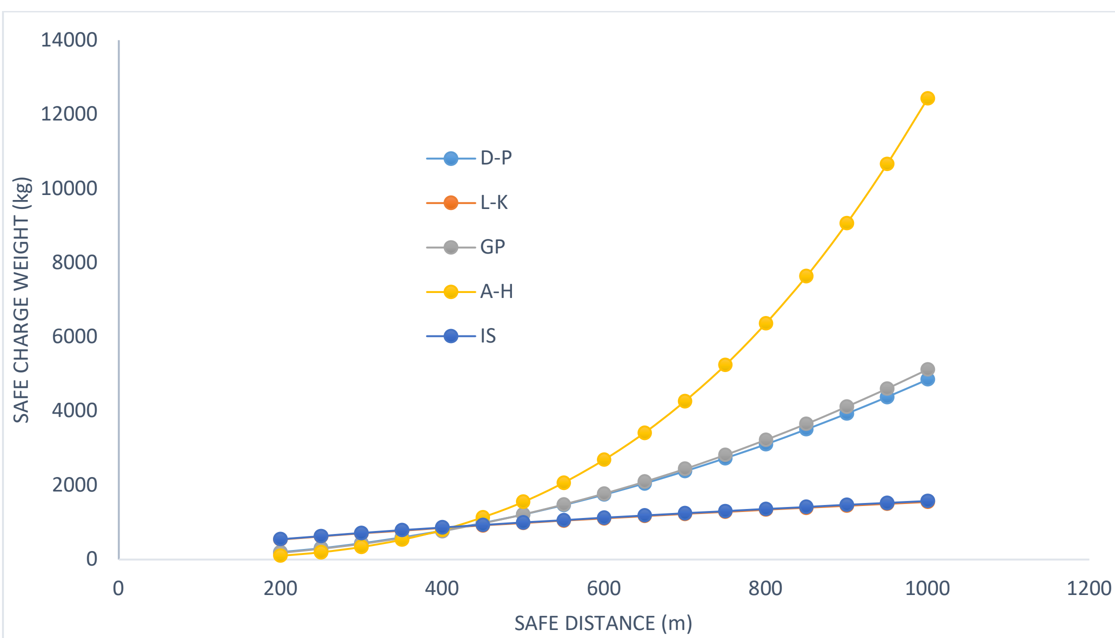

Figure 5.23 Safe charge weight distribution by various models

5.4.2.2 Correlation

The site-specific constants of rock mass are obtained using regression analysis tabulated in Table 4.2 and established attenuation Equations (4.7-4.11) by various researchers. The correlation coefficient between the scaled distance and measured peak particle velocity by various modes is 66.44%, 45.74%, 65.32%, and 45.74%, as shown in Figures 5.24, 5.25, 5.26 5.27, respectively. The various models' correlation coefficient between measured and predicted values are 74.34%, 73.75%, 74.26%, 74.28%, and 73.75%, as shown in Figures 5.28, 5.29 5.30, 5.31, and 5.32, respectively. The comparison between measured and predicted PPV values with datasets is shown in Figure 5.33.

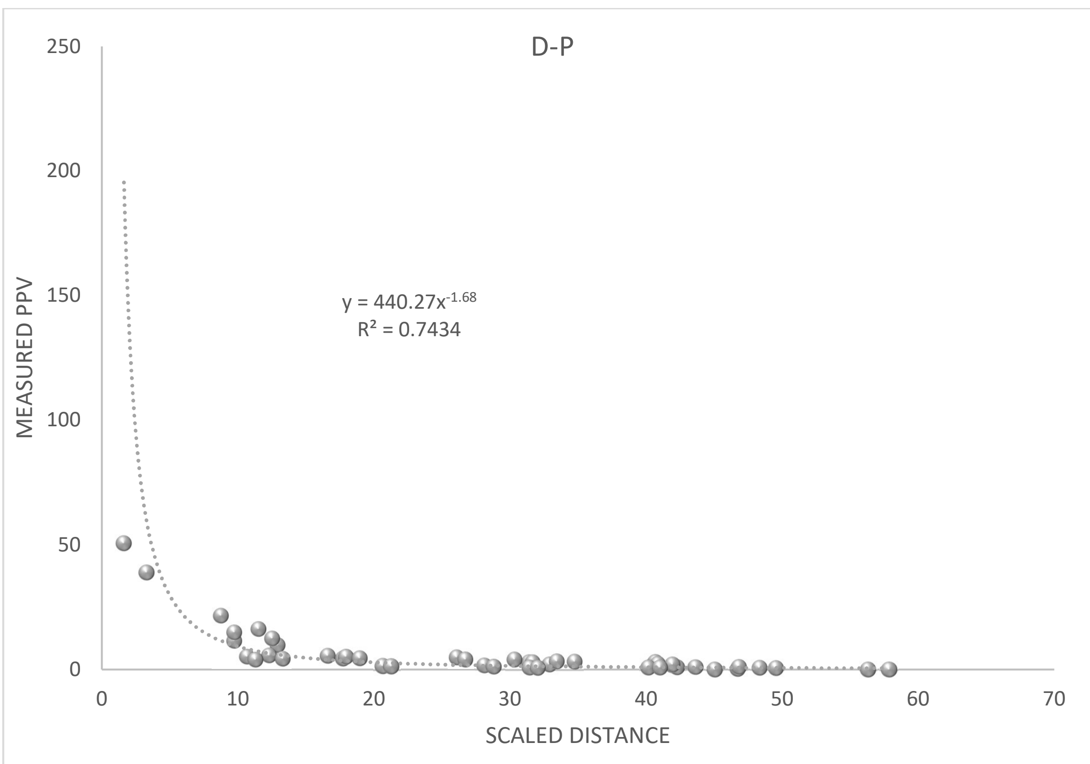

Figure 5.24 Graph plotted between SD and PPV by D-P.

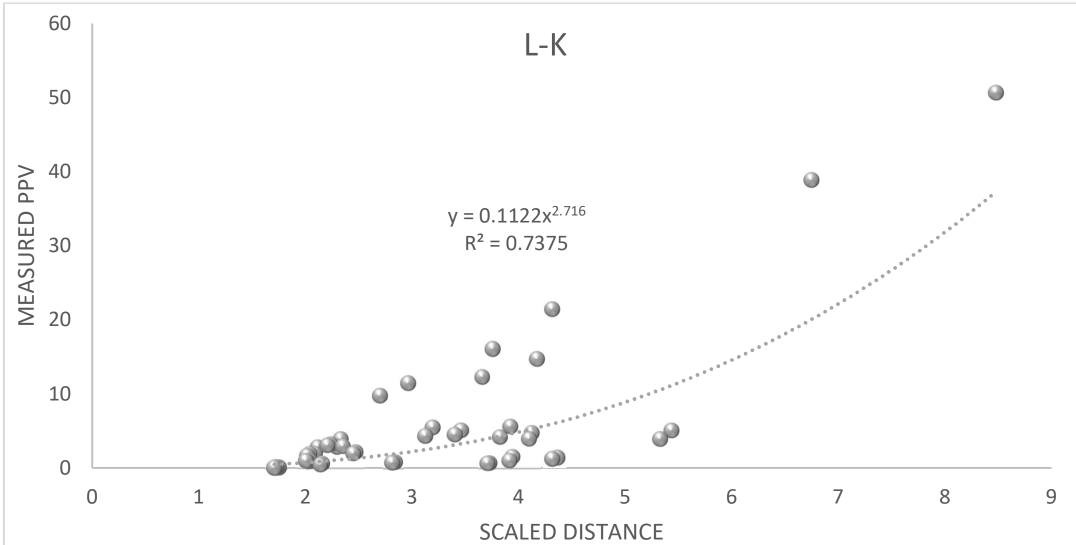

Figure 5.25 Graph plotted between SD and PPV by L-K.

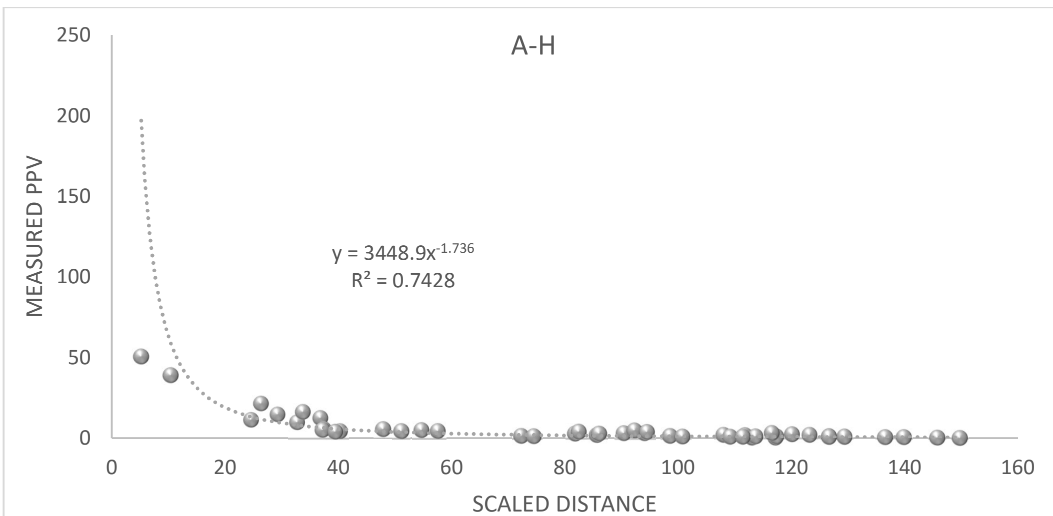

Figure 5.26 Graph plotted between SD and PPV by A-H.

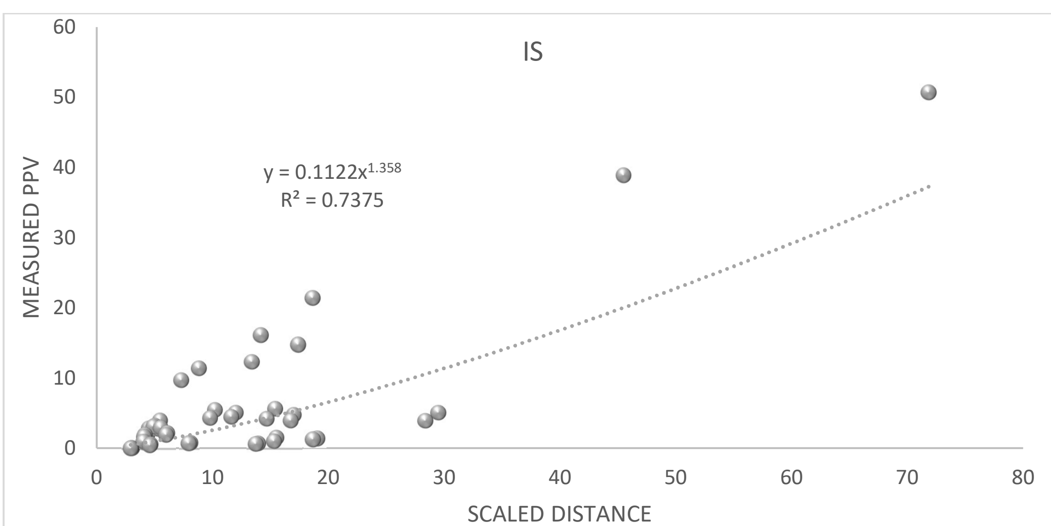

Figure 5.27 Graph plotted between SD and PPV by IS.

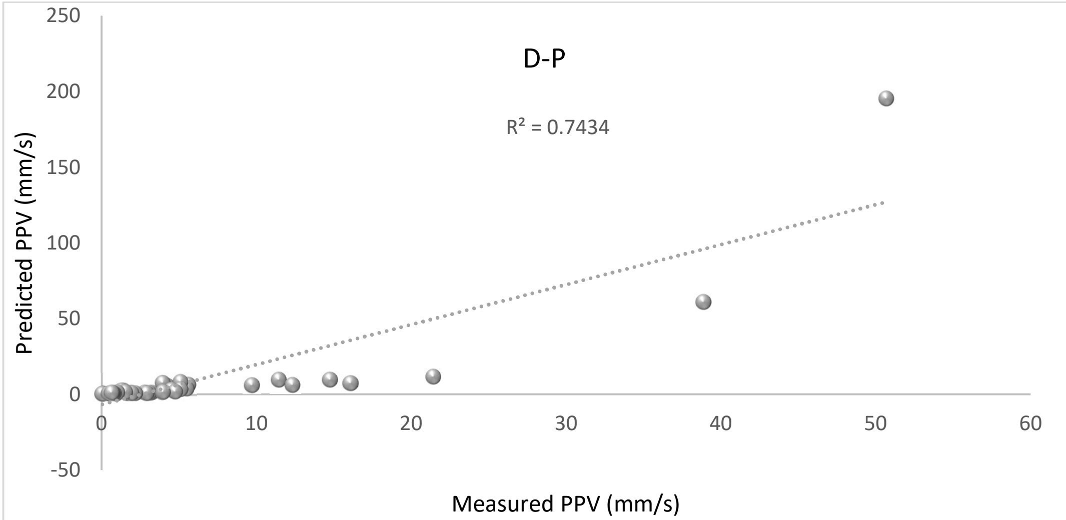

Figure 5.28 Measured and predicted PPV's correlation by D-P.

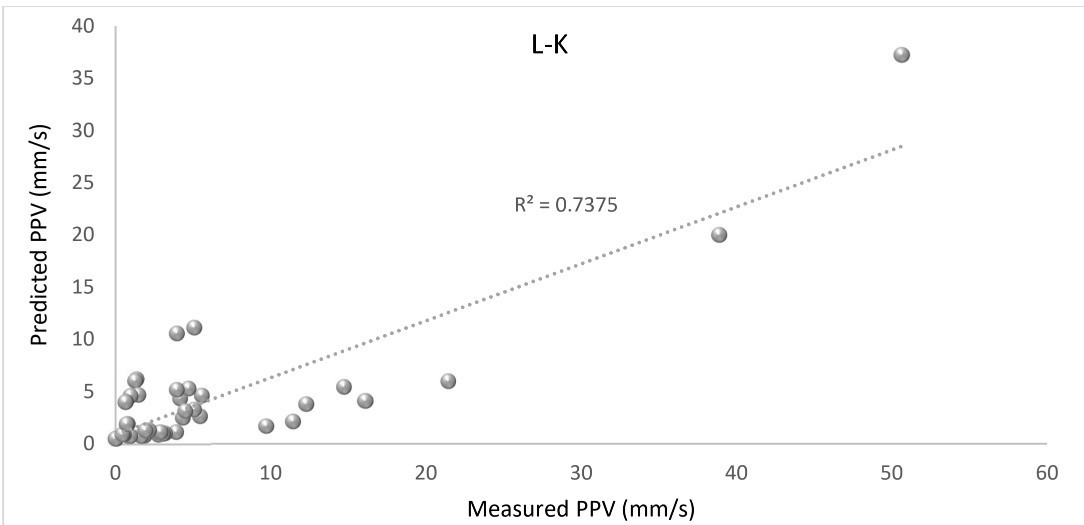

Figure 5.29 Measured and predicted PPV's correlation by L- K.

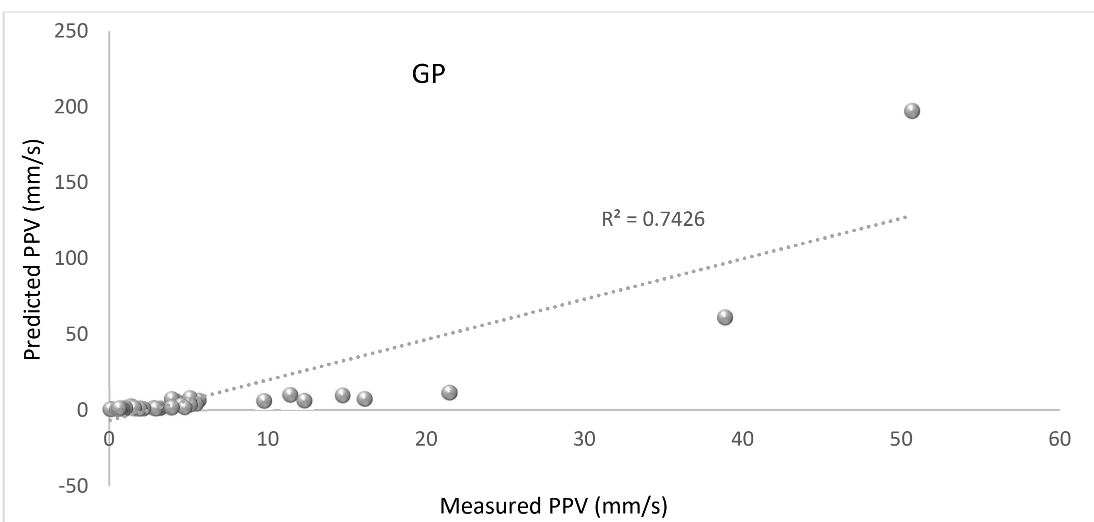

Figure 5.30 Measured and predicted PPV's correlation by GP.

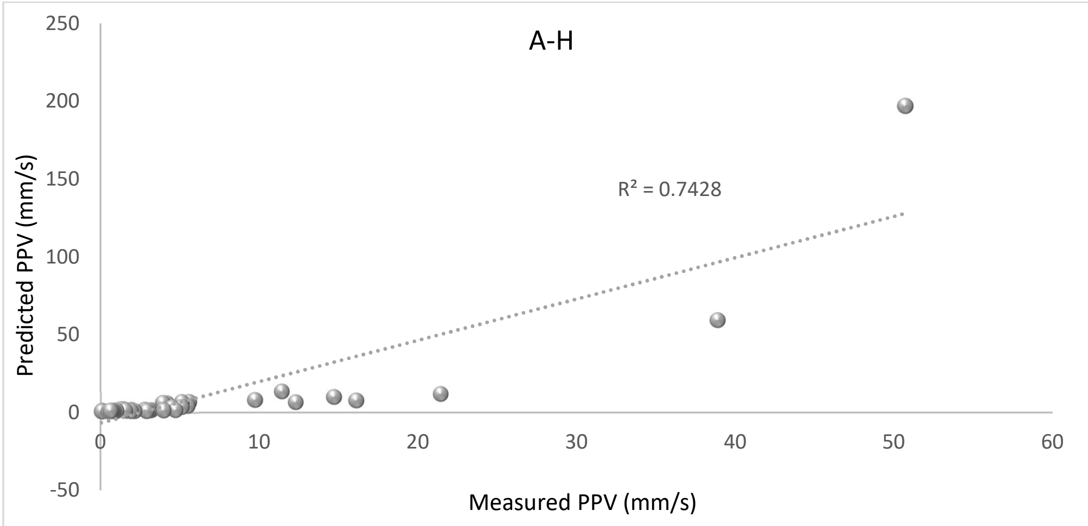

Figure 5.31 Measured and predicted PPV’s correlation by A-H.

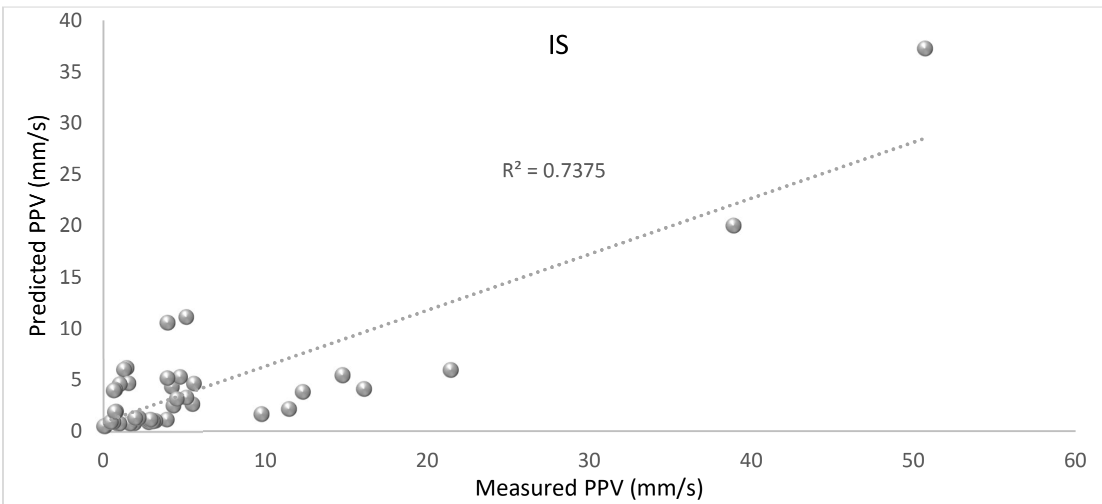

Figure 5.32 Measured and predicted PPV's correlation by IS.

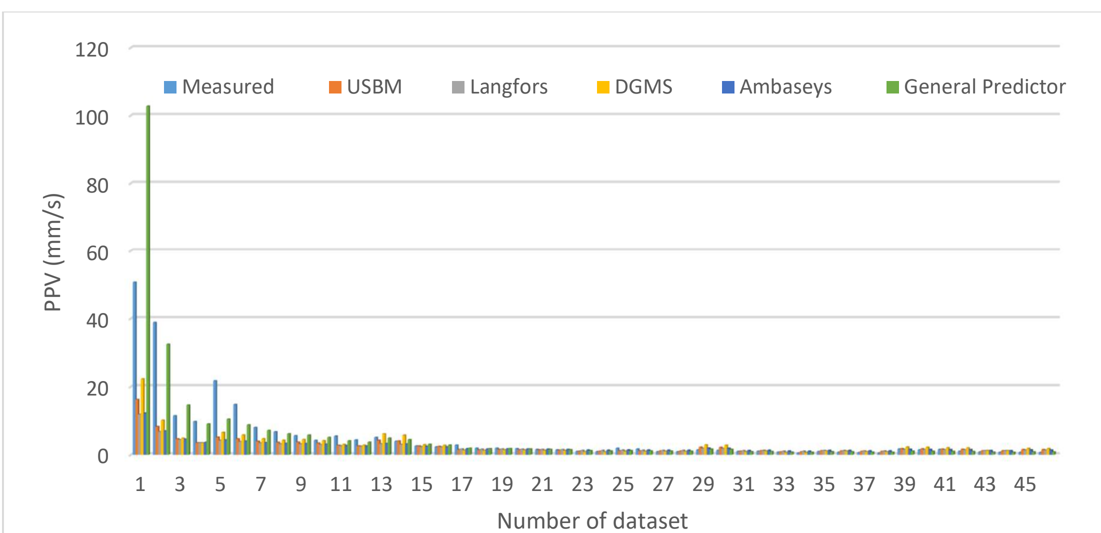

Figure 5.33 Comparison graph between measured and predicted PPV.

5.4.3 Case III: Limestone quarry-3 Chhattisgarh

The following conclusions can be drawn based on Table 3.13 for the limestone quarry-3

(i) For monitoring distance of 50m to 200m from blast site at a specific maximum charge per delay of 140kg, frequency vs. amplitude graph plotted on the logarithmic scale for orthogonal radial, transverse, vertical direction as shown in Figures 4.86 to 4.89. From these listed figures, it is evident that the density distribution of spheres is mostly above the permissible limits, which severely indicates structural damage. The peak particle velocity was obtained as 14.09 mm/s to 6.62 mm/s with the associated dominant frequency of 8.6Hz to 8.0Hz. The ground vibrations contain high-stress energy in all directions into the surface for moderate to major destruction of any structures at these distances. This may cause damage to all the structures such as domestic, industrial, and objects of historical importance, and sensitive structures should not be safe for such blast event BEN_1. Therefore, the severely destructive region is within 200 m distance from the blast site.

(ii) For monitoring distance of 250m to 400m from the blast site at a specific maximum charge per delay of 110kg, frequency vs. amplitude graph plotted on the logarithmic scale for orthogonal radial, transverse, vertical direction as shown in Figures 4.90 to 4.93. From these listed figures, it is evident that the density distribution of spheres is mostly below the permissible limits. In contrast, some are above these limits, indicating moderate structural damage. The peak particle velocity was obtained as 5.70 mm/s to 4.82 mm/s with the dominant frequency of 4.3Hz to 4.6Hz, respectively. The ground vibrations contain enough stress energy for moderate to minor damage to all the structures such as domestic, industrial, and objects of historical importance and sensitive structures and should not be safe within the distance of 400m and undergoes instant damage to the historical importance and sensitive structures for the blast event BEN_2. Beyond the distance of 350m from the blast site, PPV becomes weaker with associated dominant frequency. The region within the distance of 400m may be considered the moderate destructive region for domestic and industrial, while the severe destructive region for objects of historical importance and sensitive structures.

(iii) For monitoring distance of 450m to 600m from blast site at a specific maximum charge per delay of 75kg for blast event BEN_3, frequency vs. amplitude graph plotted on the logarithmic scale of orthogonal radial, transverse, vertical direction as shown in Figures 4.94 to 4.97. From these listed figures, it is evident that the density distribution of spheres is mostly under the permissible limits, and it indicates no instant structural damage. The peak particle velocity was obtained as 2.93 mm/s to 1.50mm/s with the associated dominant frequency as 5.7Hz to 4.6Hz, respectively. The ground vibration contains enough stress energy for moderate to minor long durational destruction due to repetitive ground vibrations to the domestic, industrial, and objects of historical importance and sensitive structures. Beyond the distance of 600m, PPV becomes weaker with associated dominant frequency. The industrial structures present within this region should be safe, while the domestic and objects of historical importance and sensitive structures may not be safe for a longer period of time. This region may be considered as a semi moderate destructive region.

(iv) For the monitoring distance of 650m to 800m from the blast site at a specific maximum charge per delay of 95kg for blast event BEN_4, frequency vs. amplitude graph plotted on the logarithmic scale for orthogonal radial, transverse, vertical direction as shown in Figures 4.98 to 4.101 From these listed figures, it is evident that the density distribution of spheres is much lower under the permissible limits and it indicates minor to threshold structural damage due to repetitively ground vibration. The peak particle velocity was obtained as 3.05mm/s to 0.78 mm/s with the associated dominant frequency of 17.6Hz to 6.7Hz, respectively. The ground vibration contains weaker stress energy and is responsible for minor to hairline damages due to the repetition of ground vibration to the domestic and sensitive structures for a longer period of time. Beyond the distance of 800m, PPV becomes much weaker with associated dominant frequency. Industrial and domestic structures should be safe within this region, while sensitive structures may not be safe for a longer time. The structures present in this region are considered to be minor destructive regions.

(v) For the monitoring distance of 850m to 1000m from the blast site at a specific maximum charge per delay of 135kg for blast event BEN_5, frequency vs. amplitude graph plotted on the logarithmic scale for orthogonal radial, transverse, vertical direction are shown in Figures 4.102 and 4.105. From these listed figures, it is evident that the density distribution of all spheres is much lower under the permissible limits, and it indicates threshold structural damage due to repetitively ground vibration. The peak particle velocity was obtained as 1.77 mm/s to 0.64 mm/s with the associated dominant frequency of 9.1Hz and 6.6Hz, respectively. The ground vibration is again much weaker and not enough for any instant damages to all types of structures. Beyond the distance of 1000m, PPV values become much weaker and weaker with associated dominant frequency at which all the structures should be safe for a much longer time. The structures present in this region are considered as threshold destructive regions.

5.4.3.1 Safe Charge Weight per Delay

In the ongoing discussion, the main objective is to find a safe charge for domestic structures like kuchcha and pukka houses near the mine site. The Indian standard proposed permissible limits for the domestic structure is 5mm/s of peak particle velocity at a frequency less than 8 Hz. It may be used to prevent damage to structures surrounding the mine site. Consideration of permissible limit of peak particle velocity is 5mm/s, and monitoring distance from the blast site enables to derive the expression for the calculation of safe charge weight per delay or maximum charge per delay is given in equation (5.7) using the data tabulated in Table 3.12. Table 5.4 shows the safe charge weight per delay with a varying distance of 50m interval. The distribution of maximum charge per delay with safe distances is shown in Figure 5.34.

$$Q_{max} = D^2 *(PPV/5.942)^{1.734} \quad (5.7)$$

Table 5.4: Obtained safe charge weight per delay

Distance (m)	Safe Charge Weight/Delay (kg)	Distance (m)	Safe Charge Weight/Delay (kg)
200	40.75	600	366.7
250	63.67	650	430.4
300	91.69	700	499.2
350	124.8	750	573
400	163	800	652
450	206.3	850	736
500	254.7	900	825.2
550	308.2	950	919.4
		1000	1018.7

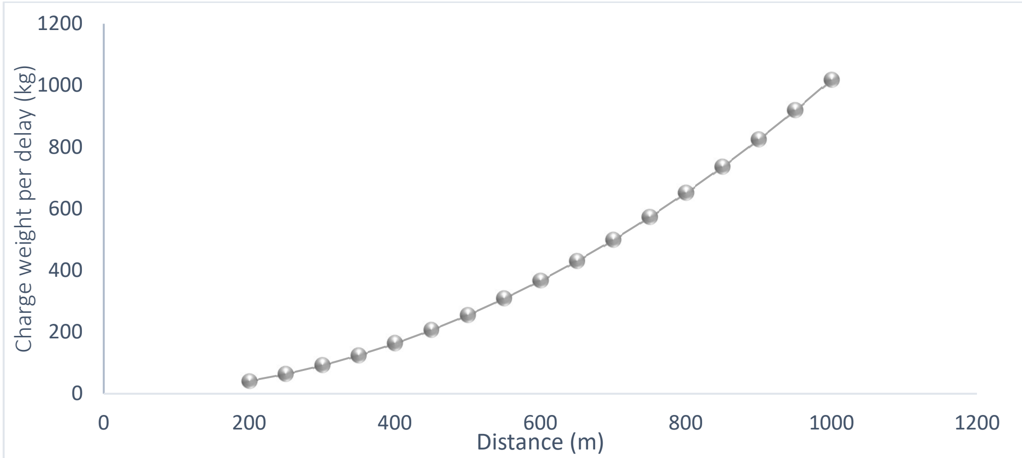

Figure 5.34 Safe charge per delay distribution

5.4.3.2 Correlation

The site-specific constant k=5.942, b=1.1532 of rock mass are obtained by using regression analysis and establishing an attenuation Equation (5.5). Find the correlation coefficient of 65.35% between the scaled distance and measured peak particle velocity as shown in figure 5.35, and it is most significant. The correlation coefficient of PPV and PVS is 65.18% and 97.63%, as shown in Figures 5.36 and 5.37, respectively. The predicted PVS is the resultant value of measured orthogonal velocities, whereas the predicted PPV depends mainly on the maximum charge per delay and monitoring distance from the blast site. The comparison between measured and predicted values of PPV, PVS with datasets and as shown in Figure 5.38 and 5.39, respectively. Velocity and frequency histogram as shown in Figure 5.40.

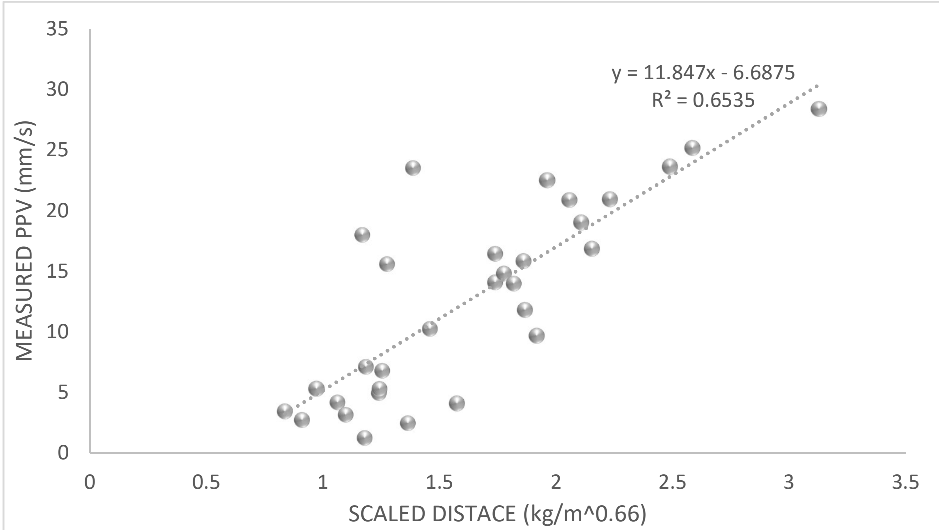

Figure 5.35 Graph plotted between scaled distance and measured PPV.

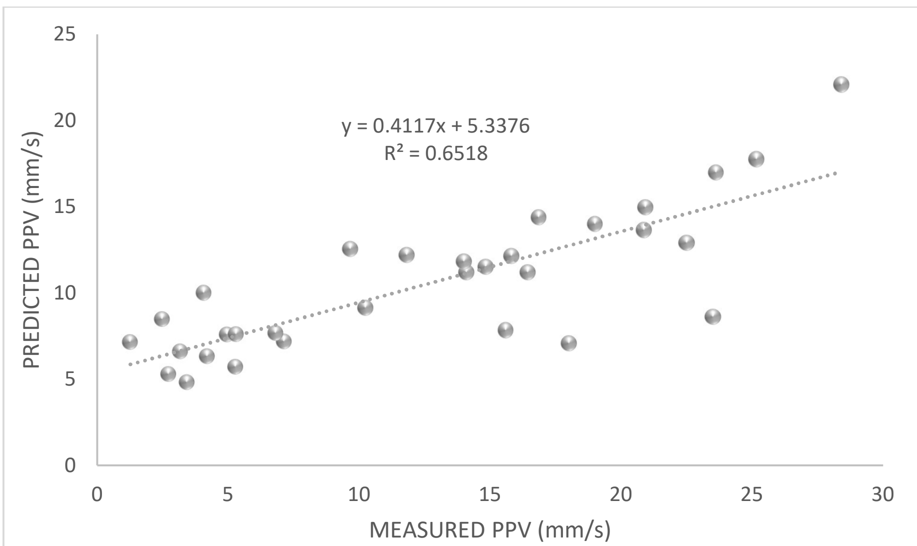

Figure 5.36 Graph plotted between measured and predicted PPV.

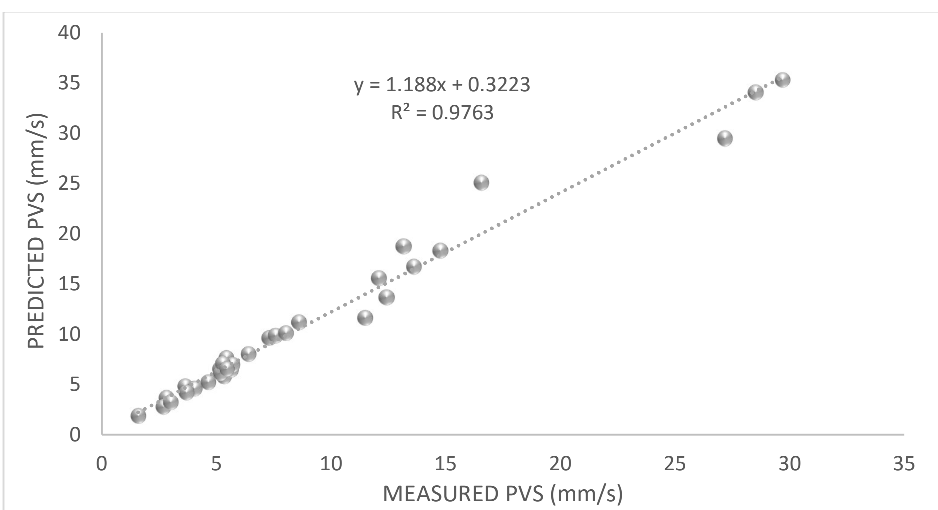

Figure 5.37 Graph plotted between measured and predicted PVS.

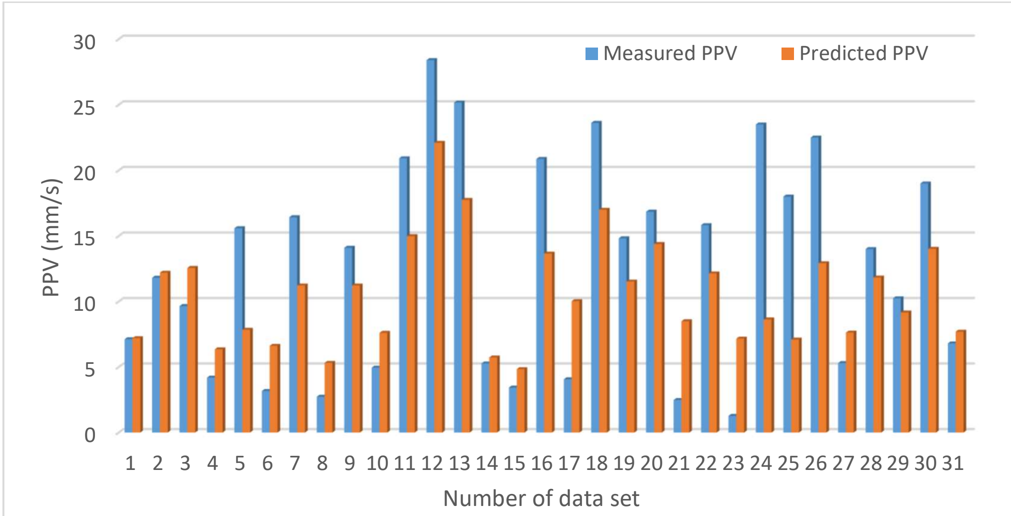

Figure 5.38 Wavelets of measured and predicted PPV with datasets

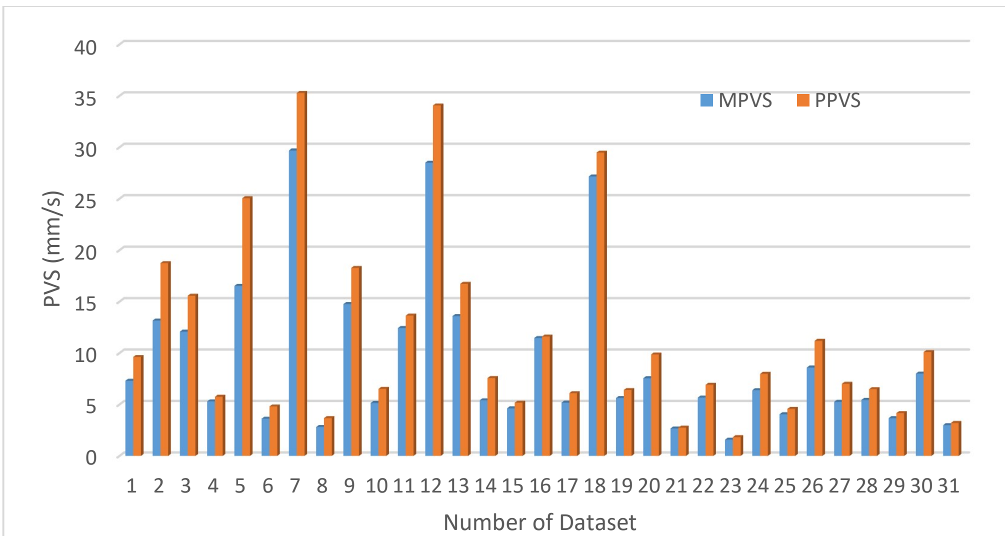

Figure 5.39 Wavelets of PPV and PVS with datasets

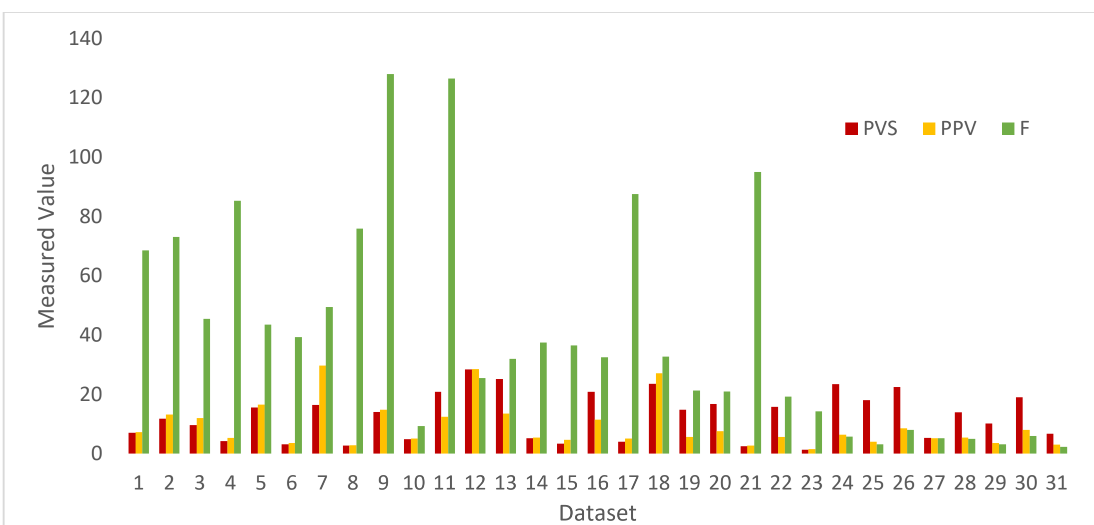

Figure 5.40 Velocity and frequency building histogram with datasets

5.4.4 Case IV: Stone quarry-4 Bihar

Based on Table 3.14 for stone quarry-4, the following conclusions can be drawn.

(i) For monitoring distance of 50m to 200m from blast site at a specific maximum charge per delay of 210kg, frequency vs. amplitude graph plotted on the logarithmic scale for orthogonal radial, transverse, vertical direction as shown in Figures 4.108 to 4.111. From these listed figures, it is evident that the density distribution of spheres is mostly above the permissible limits, which severely indicates structural damage. The peak particle velocity was obtained as 25.02 mm/s to 11.43 mm/s with the dominant frequency of 3.4Hz to 3.3Hz. The ground vibrations contain high-stress energy in all directions into the surface for moderate to major destruction of any type of structures at these distances. This may cause damage to all the structures such as domestic, industrial, and objects of historical importance and sensitive structures should not be safe for such blast event BEN_1. Therefore, the severely destructive region is within 200 m distance from the blast site.

(ii) For monitoring distance of 250m to 400m from the blast site at a specific maximum charge per delay of 195kg, frequency vs. amplitude graph plotted on the logarithmic scale for orthogonal radial, transverse, vertical direction as shown in Figures 4.112 to 4.115. From these listed figures, it is evident that the density distribution of spheres is mostly below the permissible limits, whereas some are above these limits, and it indicates moderate structural damage. The peak particle velocity was obtained as 8.90 mm/s to 4.56 mm/s with the dominant frequency of 56.8Hz to 46.5Hz, respectively. The ground vibrations contain enough stress energy for moderate to minor damage to all the structures such as domestic, industrial, and objects of historical importance and sensitive structures and should not be safe within the distance of 400m and undergoes instant damage to the historical importance and sensitive structures for the blast event BEN_2. Beyond the distance of 400m from the blast site, PPV becomes weaker with associated dominant frequency. The region within distance of 400m may be considered a moderate destructive region for domestic and industrial while a severe destructive region for objects of historical importance and sensitive structures.

(iii) For monitoring distance of 450m to 600m from blast site at a specific maximum charge per delay of 145kg for blast event BEN_3, frequency vs. amplitude graph plotted on the logarithmic scale of orthogonal radial, transverse, vertical direction as shown in Figures 4.116 to 4.119. From these listed figures, it is evident that the density distribution of spheres is mostly under the permissible limits, and it indicates no instant structural damage. The peak particle velocity was obtained as 2.66mm/s to 0.760 mm/s with the associated dominant frequency of 8.3Hz to 19.6Hz, respectively. The ground vibration contains enough stress energy for moderate to minor long durational destruction due to repetitive ground vibration to the domestic, industrial, and objects of historical importance and sensitive structures. Beyond the distance of 600m, PPV becomes weaker with the associated dominant frequency. The industrial structures present within this region should be safe, while the domestic and objects of historical importance and sensitive structures may not be safe for a longer period of time. This region may be considered as a semi moderate destructive region.

(iv) For the monitoring distance of 650m to 800m from the blast site at a specific maximum charge per delay of 110kg for blast event BEN_4, frequency vs. amplitude graph plotted on the logarithmic scale for orthogonal radial, transverse, vertical direction as shown in Figures 4.120 to 4.123. From these listed figures, it is evident that the density distribution of spheres is much lower under the permissible limits, and it indicates minor to threshold structural damage due to repetitively ground vibration. The peak particle velocity was obtained as 1.43 mm/s to 0.635mm/s with the associated dominant frequency of 24.7Hz to 28.0Hz, respectively. The ground vibration contains weaker stress energy and is responsible for minor to hairline damages due to the repetition of ground vibration to the domestic and sensitive structures for a longer period of time. Beyond the distance of 800m, PPV becomes much weaker with associated dominant frequency. Industrial and domestic structures should be safe within this region, while sensitive structures may not be safe for a longer period of time. The structures present in this region are considered to be minor destructive regions.

(v) For the monitoring distance of 850m to 1000m from the blast site at a specific maximum charge per delay of 90kg for blast event BM_5, frequency vs. amplitude graph plotted on the logarithmic scale for orthogonal radial, transverse, vertical direction as shown in Figures 4.124 and 4.127. From these listed figures, it is evident that the density distribution of all spheres is much lower under the permissible limits, and it indicates threshold structural damage due to repetitively ground vibration. The peak particle velocity was obtained as 1.016 mm/s to 0.60 mm/s with the associated dominant frequency 3.5Hz and 2.7Hz, respectively. The ground vibration is again much weaker and not enough for any instant damages to all types of structures. Beyond the distance of 1000m, PPV values become much weaker and weaker with associated dominant frequency at which all the structures should be safe for a much longer time. The structures present in this region are considered as threshold destructive regions.

5.4.4.1 Safe Charge Weight

In the ongoing discussion, the main objective is to find a safe charge for domestic structures like kuchcha and pukka houses near the mine site. The Indian standard proposed permissible limits for the domestic structure is to 5mm/s of peak particle velocity at a frequency less than 8 Hz. It may be used to prevent damage to structures surrounding the mine site. Consideration of permissible limit of peak particle velocity is 5mm/s, and monitoring distance from the blast site enables to derive the expression for the calculation of safe charge weight per delay or maximum charge per delay is given in Equation (5.7) using the data tabulated in

Table 3.16. Table 5.5 shows the safe charge weight per delay with a varying distance of 100m interval. The distribution of maximum charge per delay with safe distances, as shown in Figure 5.41.

$$Q_{max} = D^{0.66} * (PPV/0.5597)^{0.668} \quad (5.7)$$

Table 5.5: Safe charge weight distribution

Distance (m)	Safe Charge Weight/Delay (kg)	Distance (m)	Safe Charge Weight/Delay (kg)
200	142.54	1200	465.09
300	186.28	1300	490.32
400	225.23	1400	514.89
500	260.97	1500	538.88
600	294.34	1600	562.33
700	325.86	1700	585.29
800	355.89	1800	607.79
900	384.66	1900	629.87
1000	412.36	2000	651.56
1100	439.13		

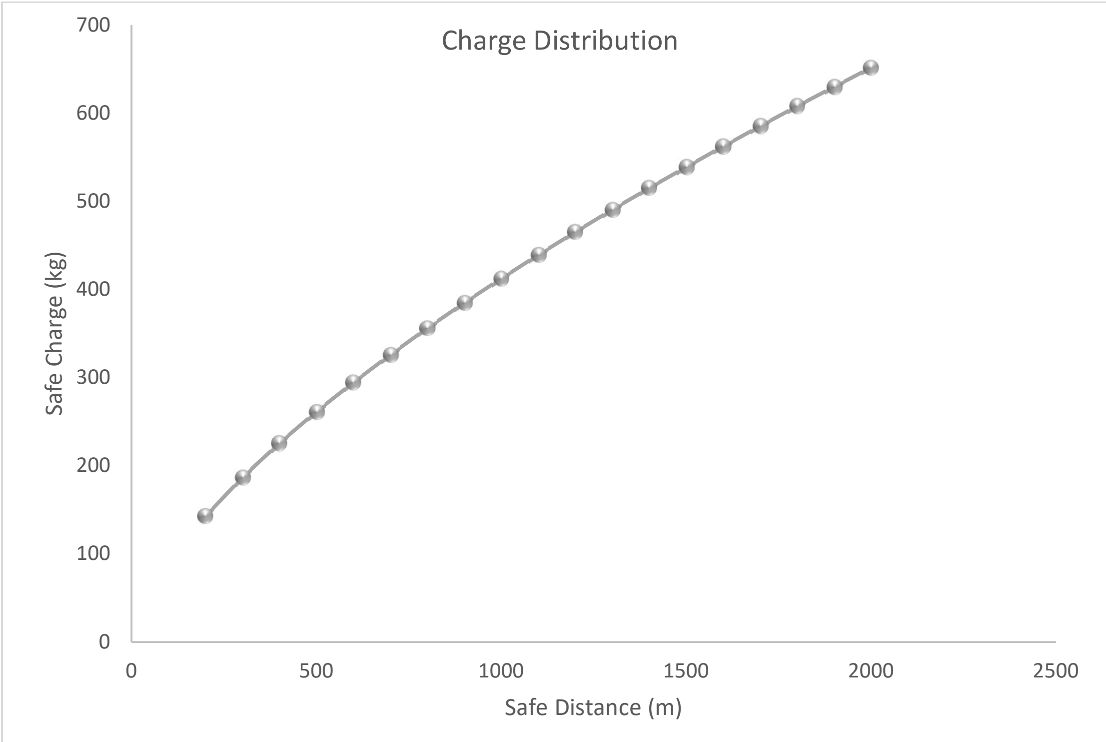

Figure 5.41 Safe charge per delay distribution

5.4.4.2 Correlation

The site-specific constant k=137.16 and 0.5597, b= -1.073 and 1.497 of rock mass are described in Equations (5.8) and (5.9) for USBM and IS, respectively. The most significant correlation coefficient of 83.43% and 91.08%, as shown in Figures 5.42 and 5.43, respectively. The most significant correlation coefficient between measured and predicted PPV is 87.72% and 90.43%, by USBM and IS, as shown in Figures 5.44 and 5.45, respectively.

$$PPV = 137.16 * (D/Q_{max}^{0.5})^{-1.073} \quad (5.8)$$

$$PPV = 0.5597 * (Q_{max}/D^{0.66})^{1.497} \quad (5.9)$$

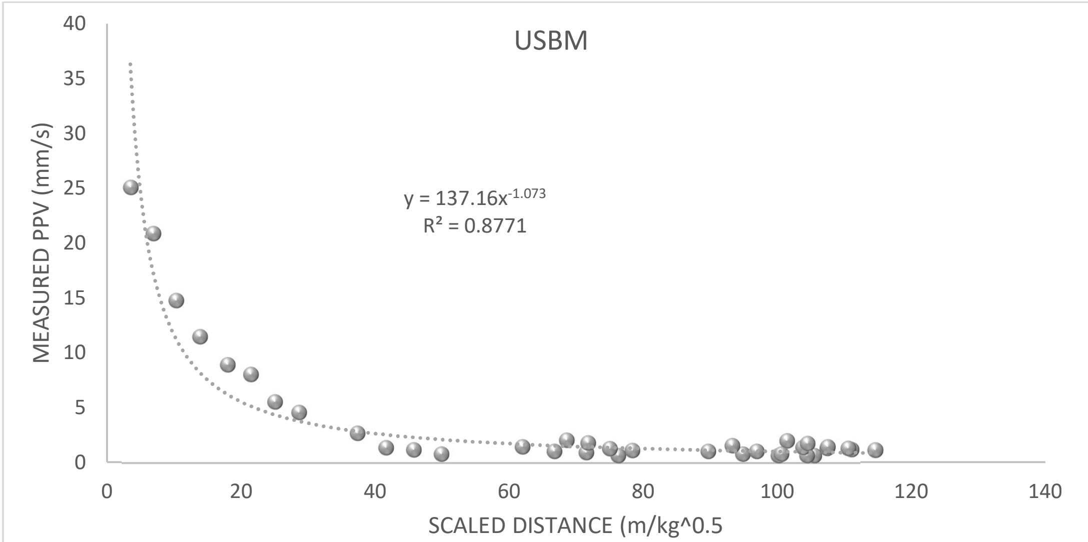

Figure 5.42 Graph plotted between SD and PPV of USBM.

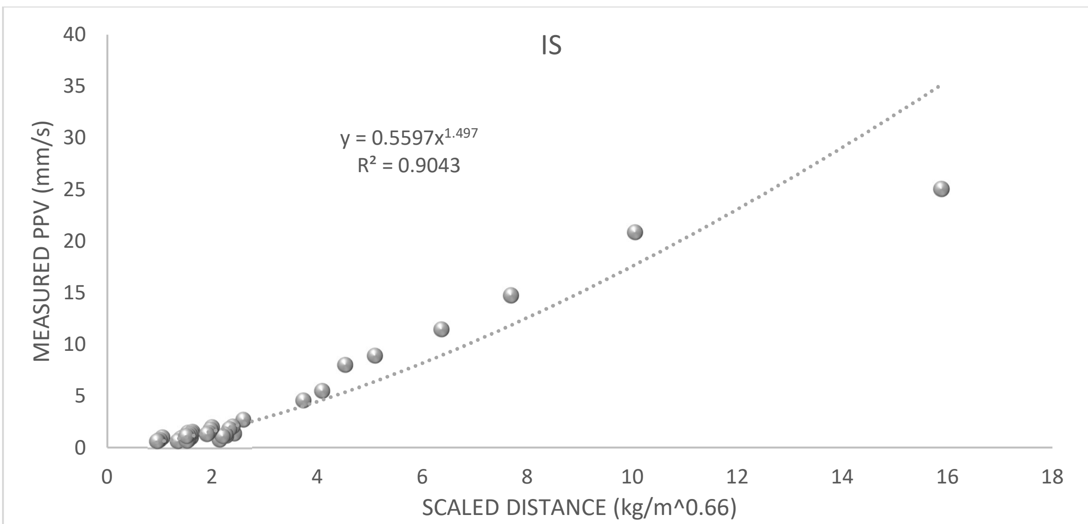

Figure 5.43 Graph plotted between SD and PPV by IS.

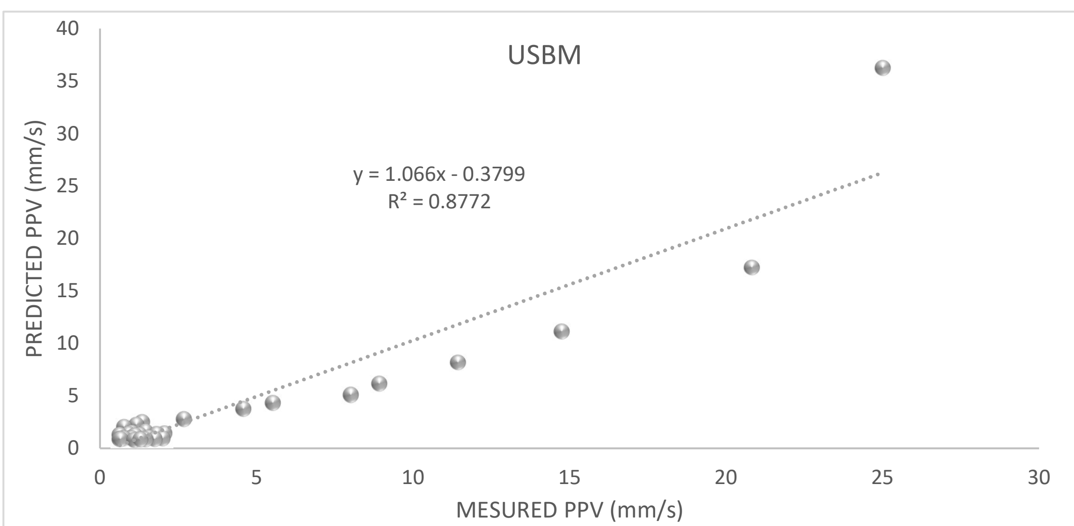

Figure 5.44 Graph plotted between measured and predicted PPV.

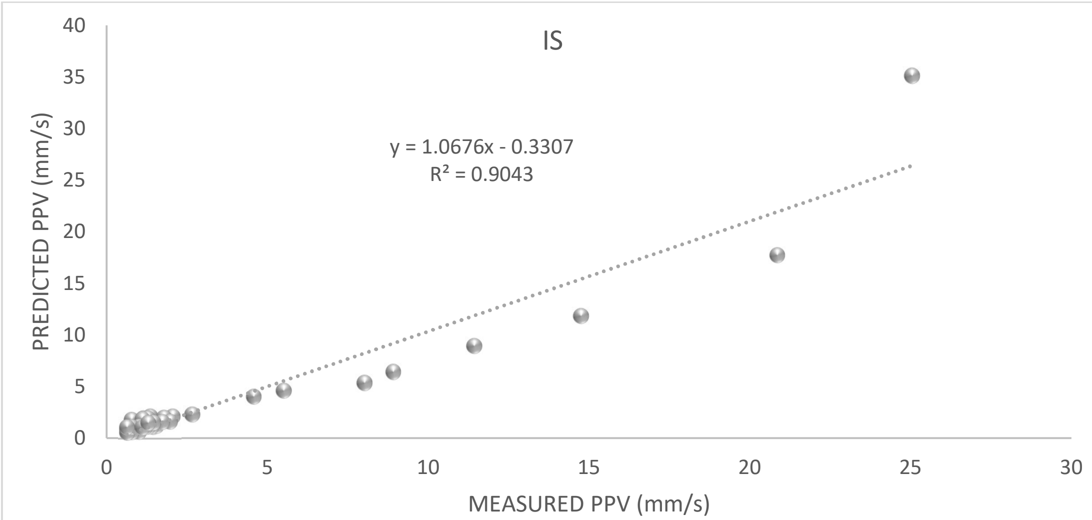

Figure 5.45 Graph plotted between measured and predicted PPV

5.4.5 Case V: Stone quarry-5 Uttar Pradesh

The following conclusions can be drawn based on Table 3.17 for the Stone quarry-5

(i) For monitoring distance of 50m to 200m from blast site at a specific maximum charge per delay of 160kg, frequency vs. amplitude graph plotted on the logarithmic scale for orthogonal radial, transverse, vertical direction as shown in Figures 4.128 to 4.131. From these listed figures, it is evident that the density distribution of spheres is mostly above the permissible limits, which severely indicates structural damage. The peak particle velocity was obtained as 21.20 mm/s to 9.2 mm/s with the associated dominant frequency of 56Hz to 3.7Hz. The ground vibrations contain high-stress energy in all directions into the surface for moderate to major destruction of any type of structures at these distances. This may cause damage to all the structures such as domestic, industrial, and objects of historical importance, and sensitive structures should not be safe for such blast event BM_1. Therefore, the severely destructive region is within 200 m distance from the blast site.

(ii) For monitoring distance of 250m to 400m from the blast site at a specific maximum charge per delay of 225kg, frequency vs. amplitude graph plotted on the logarithmic scale for orthogonal radial, transverse, vertical direction as shown in Figures 4.132 to 4.135. From these listed figures, it is evident that the density distribution of spheres is mostly below the permissible limits. In contrast, some are above these limits, and it indicates moderate structural damage. The peak particle velocity was obtained as 10.29 mm/s to 5.20 mm/s with the dominant frequency of 1.5 Hz to 23.2Hz, respectively. The ground vibrations contain enough stress energy for moderate to minor damage to all the structures such as domestic, industrial, and objects of historical importance and sensitive structures and should not be safe within the distance of 350m and undergoes instant damage to the historical importance and sensitive structures for the blast event $BEN_{2.}$ Beyond the distance of 400m from the blast site, PPV becomes weaker with associated dominant frequency. The region within the distance of 400m may be considered the moderate destructive region for domestic and industrial, while the severe destructive region for objects of historical importance and sensitive structures.

(iii) For monitoring distance of 450m to 600m from blast site at a specific maximum charge per delay of 124kg for blast event BEN_3, frequency vs. amplitude graph plotted on the logarithmic scale of orthogonal radial, transverse, vertical direction as shown in Figures 4.136 to 4.139. From these listed figures, it is evident that the density distribution of spheres is mostly under the permissible limits, and it indicates no instant structural damage. The peak particle velocity was obtained as 2.67 mm/s to 0.89mm/s with the associated dominant frequency of 1.6Hz to 4.3Hz, respectively. The ground vibration contains enough stress energy for moderate to minor long durational destruction due to repetitive ground vibration to the domestic, industrial, and objects of historical importance and sensitive structures. Beyond the distance of 600m, PPV becomes weaker with associated dominant frequency. The industrial structures present within this region should be safe, while the domestic and objects of historical importance and sensitive structures may not be safe for a longer period of time. This region may be considered as a semi moderate destructive region.

(iv) For the monitoring distance of 650m to 800m from the blast site at a specific maximum charge per delay of 190kg for blast event BEN_4, frequency vs. amplitude graph plotted on the logarithmic scale for orthogonal radial, transverse, vertical direction as shown in Figures 4.140 to 4.143. From these listed figures, it is evident that the density distribution of spheres is much lower under the permissible limits, and it indicates minor to threshold structural damage due to repetitively ground vibration. The peak particle velocity was obtained as 4.32 mm/s to 1.02 mm/s with the associated dominant frequency of 11.3Hz to 2.5Hz, respectively. The ground vibration contains weaker stress energy and is responsible for minor to hairline damages due to the repetition of ground vibration to the domestic and sensitive structures for a longer period of time. Beyond the distance of 800m, PPV becomes much weaker with associated dominant frequency. Industrial and domestic structures should be safe within this region, while sensitive structures may not be safe for a longer period of time. The structures present in this region are considered to be minor destructive regions.

(v) For the monitoring distance of 850m to 1000m from the blast site at a specific maximum charge per delay of 215kg for blast event BEN_5, frequency vs. amplitude graph plotted on the logarithmic scale for orthogonal radial, transverse, vertical direction as shown in Figures 4.144 and 4.147. From these listed figures, it is evident that the density distribution of all spheres is much lower under the permissible limits, and it indicates threshold structural damage due to repetitively ground vibration. The peak particle velocity was obtained as 1.9 mm/s to 0.762 mm/s with the associated dominant frequency of 4.8Hz and 39.2Hz, respectively. The ground vibration is again much weaker and not enough for any instant damages to all types of structures. Beyond the distance of 1000m, PPV values become much weaker and weaker with associated dominant frequency at which all the structures should be safe for a much longer time. The structures present in this region are considered as threshold destructive regions.

5.4.5.1 Safe Charge Weight per Delay

In the ongoing discussion, the main objective is to find a safe charge for domestic structures like kuchcha and pukka houses near the mine site. The Indian standard proposed permissible limits for the domestic structure are 5mm/s of peak particle velocity at less than 8 Hz. It may be used to prevent damage to structures surrounding the mine site. Consideration of permissible limit of peak particle velocity 5mm/s and monitoring distance from the blast site enables to derive the expression for the calculation of safe charge weight per delay or maximum charge per delay is given in Equation (5.10) using the data tabulated in Table 3.18. Table 5.6 shows the safe charge weight per delay with a varying distance of 100m interval. The distribution of maximum charge per delay with safe distances is shown in Figure 5.46.

$$Q_{max} = D^{0.66} * (PPV/0.4167)^{0.570} \quad (5.10)$$

Table 5.6: Safe charge weight distribution

Distance (m)	Safe Charge Weight/Delay (kg)	Distance (m)	Safe Charge Weight/Delay (kg)
200	136.07	1200	443.98
300	177.83	1300	468.07
400	215.01	1400	491.54
500	249.13	1500	514.43
600	280.99	1600	536.82
700	311.08	1700	558.74
800	339.74	1800	580.22
900	367.20	1900	601.29
1000	393.65	2000	622.00
1100	419.211		

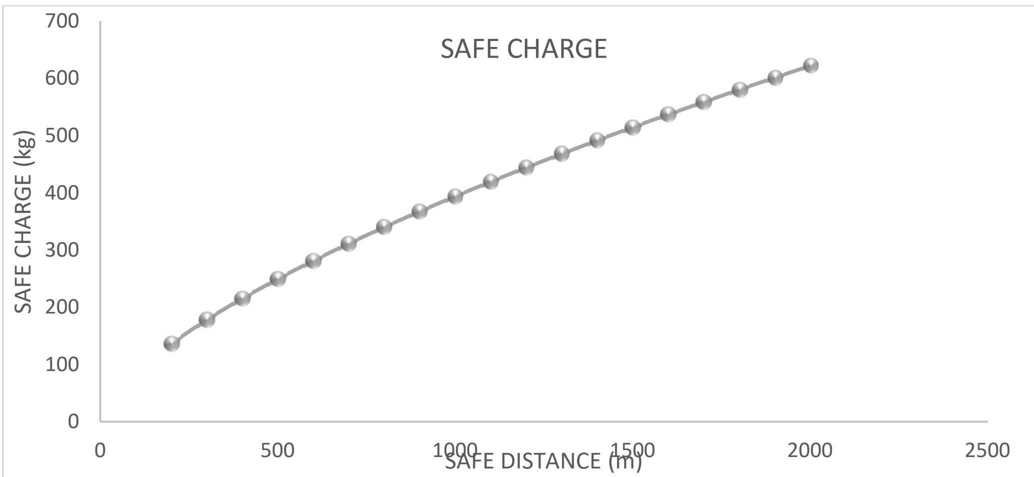

Figure 5.46 Safe charge per delay distribution

5.4.4.2 Correlation

The site-specific constant k=132.66 and 0.4168, b= -1.034 and 1.754 of rock mass are described in Equations (5.11) and (5.12) for USBM and IS, respectively. The most significant correlation coefficient is 80.97% and 84.13%, as shown in Figures 5.47 and 5.48. The most significant correlation coefficient between measured and predicted PPV is 86.44% and 85.73%, for USBM and IS, as shown in Figures 5.49 and 5.50, respectively.

$$PPV = 132.66 * (D/Q_{max}^{0.5})^{-1.034} \quad (5.11)$$

$$PPV = 0.4168 * (Q_{max}/D^{0.66})^{1.754} \quad (5.12)$$

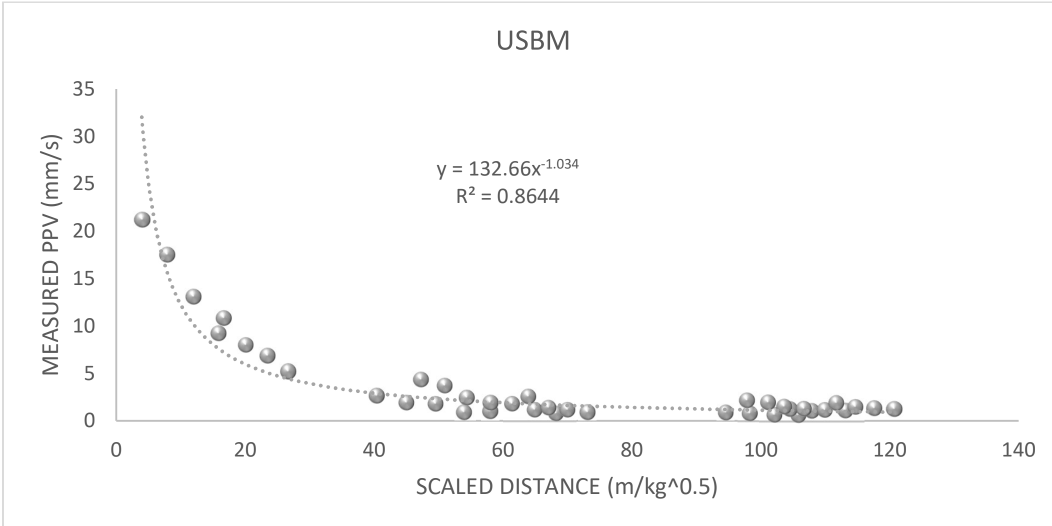

Figure 5.47 Graph plotted between SD and PPV by USBM.

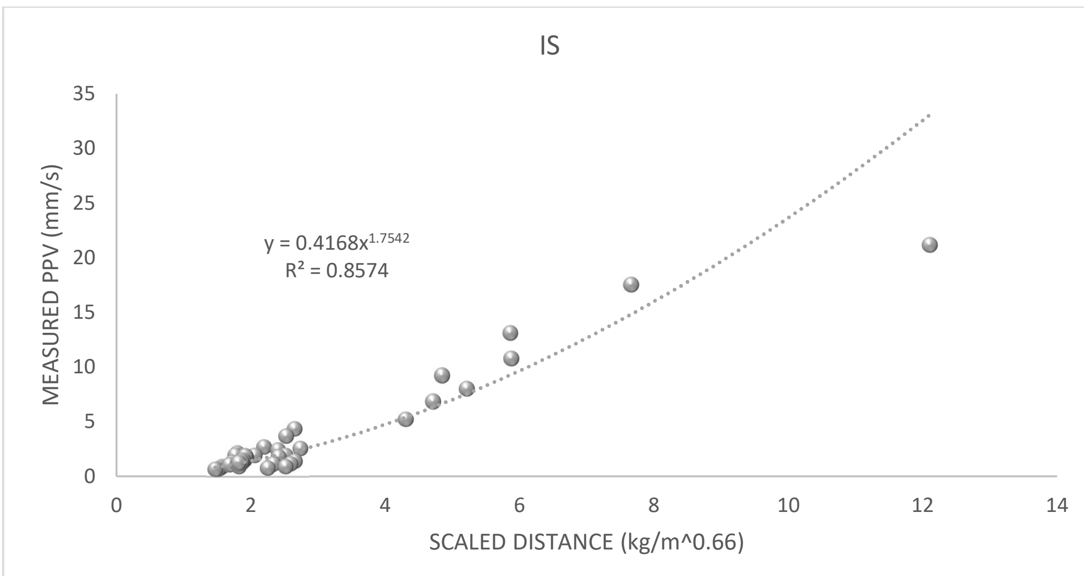

Figure 5.48 Graph plotted between SD and PPV by IS.

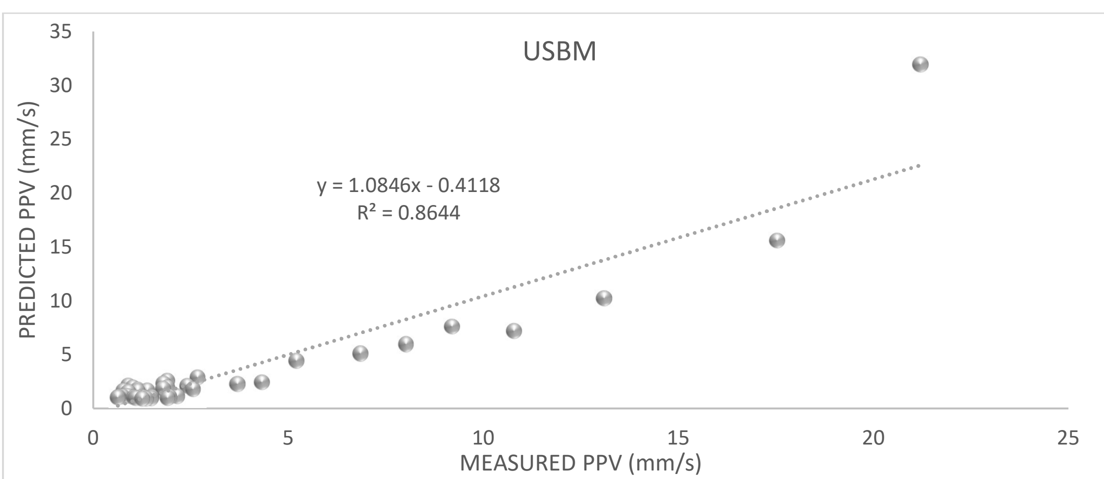

Figure 5.49 Graph plotted between measured and predicted PPV.

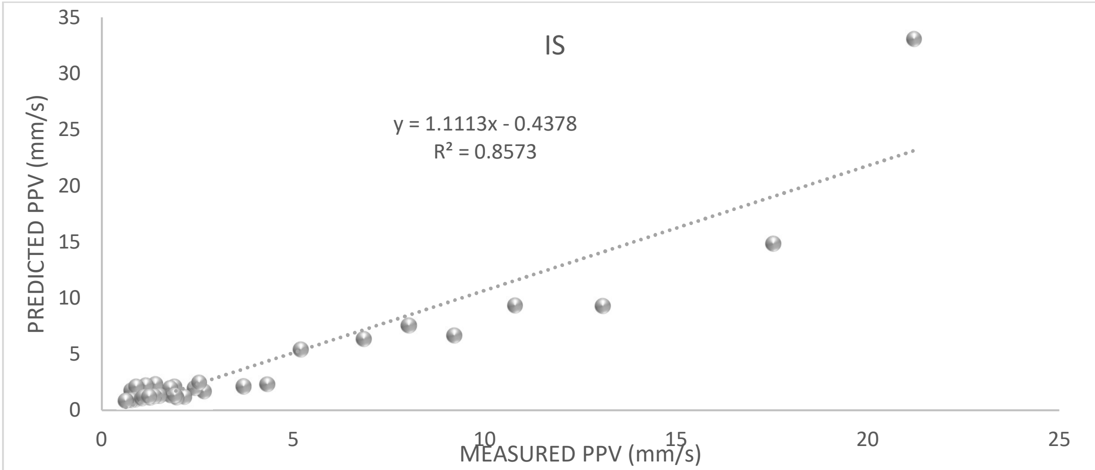

Figure 5.50 Graph plotted between measured and predicted PPV

Based on the above results and discussions, a comparative table had been prepared for the safe charge per delay, structural response, and correlation coefficients, and various predictor formulae for all the considered case study.

Table 5.7: Safe charge per delay for various mine and quarry.

Distance (m)	**Case I** (Coal mine-1)	**Case II** (Coal mine-2)					**Case III** (Limestone quarry-3)	**Case IV** (Stone quarry-4)	**Case V** (Stone quarry-5)
	Q_{max} IS	**Q_{max}** D-K	**Q_{max}** L-K	**Q_{max}** GP	**Q_{max}** A-H	**Q_{max}** IS	**Q_{max}** USBM	**Q_{max}** IS	**Q_{max}** IS
300	203	436	701	419	335	712	91	186	177
500	285	1213	983	1213	1554	998	254	260	249
800	389	3106	1340	3224	6367	1361	652	356	339
1000	451	4853	1553	5127	12436	1577	1018	412	393

Table 5.8: Structural response at given distances for various mine and quarry.

Distance (m)	Case I (Coal mine-1)			Case II (Coal mine-2)			Case III (Limestone quarry -3)			Case IV (Stone quarry -4)			Case V (Stone quarry -5)		
	Q_{max} kg	PPV mm/s	f Hz	Q_{max} kg	PPV mm/s	f Hz	Q_{max} kg	PPV mm/s	f Hz	Q_{max} kg	PPV mm/s	f Hz	Q_{max} kg	PPV mm/s	f Hz
300	280	5.33	3.8	645	6.73	20.4	110	5.45	5.7	195	8.0	56.8	225	8.0	6.4
500	324	4.06	4.3	704	4.45	36.5	75	2.41	4.6	145	1.34	6.8	124	1.9	14.2
800	475	1.55	28.0	540	1.53	3.7	95	0.76	6.7	110	0.64	3.7	190	1.02	2.5
1000	470	1.14	6.10	815	1.02	12.8	80	0.64	6.6	90	0.63	2.7	215	0.76	39.2

Table 5.9: Correlation coefficients for various mine and quarry by different models.

		Case I (Coal Mine-1)			Case II (Coal Mine-2)					Case III (Lime stone quarry -3)	Case IV (Stone quarry-4)		Case V (Stone quarry-5)	
		IS	MVRA	ANN	D-K	L-K	GP	A-H	IS	IS	USBM	IS	USBM	IS
Correlation Coefficient (%)	M/P (PPV)	72.90	75.76	92.04	74.34	73.75	74.26	74.28	73.75	65.18	87.72	90.4	86.44	85.73
	M/P (frequency)	-	26.0	60.65	-	-	-	-	-	-	-	-	-	-
	SD/PPV	83.37	-	-	66.44	45.74	-	65.32	45.74	65.35	83.43	91.0	80.97	84.13
	f/PPV	-	-	62.67	-	-	-	-	-	-	-	-	-	-